NASA TECHNICAL NOTE

NASA TN D-5114

NASA TN D-5114

LOW-DENSITY FOAM FOR INSULATING LIQUID-HYDROGEN TANKS

by Irving E. Sumner

Lewis Research Center

Cleveland, Ohio

NATIONAL AERONAUTICS AND SPACE ADMINISTRATION • WASHINGTON, D. C. • MARCH 196

12265

NASA TN D-5114

LOW-DENSITY FOAM FOR INSULATING LIQUID-HYDROGEN TANKS

By Irving E. Sumner

Lewis Research Center
Cleveland, Ohio

NATIONAL AERONAUTICS AND SPACE ADMINISTRATION

For sale by the Clearinghouse for Federal Scientific and Technical Information
Springfield, Virginia 22151 – CFSTI price $3.00

ABSTRACT

A lightweight polyurethane foam insulation for liquid hydrogen tanks of space vehicles was developed that (1) could be foamed in place, (2) did not crack when chilled to liquid hydrogen temperature, and (3) had a thermal conductivity of 0.0137 W/(m)(K) (0.0079 Btu/(hr)(ft)(^{o}R)) at a mean temperature of 136 K (243^{o} R). The foaming-in-place technique in which the foam constituents were poured directly on the tank, coupled with the specific foam formulation, produced a 34.4-kg/m^{3} (2.14-lb/ft^{3}) density foam that remained structurally intact during all simulated ground-hold, vibration, and space-hold tests conducted. Thermophysical properties of the foam were determined, and thermal stress profiles throughout a layer of insulation were calculated.

LOW-DENSITY FOAM FOR INSULATING LIQUID-HYDROGEN TANKS

by Irving E. Sumner

Lewis Research Center

SUMMARY

The objective of this investigation was to develop and test a lightweight polyurethane foam insulation for liquid hydrogen tanks of space vehicles that (1) could be foamed in place on the outside of the tank, (2) would not require any strengthening or reinforcing to prevent cracking and splitting when chilled to liquid hydrogen temperature, and (3) would have a thermal conductivity of approximately 0.015 watt per meter per K (0.0087 Btu/(hr)(ft)(^{o}R)) at a mean temperature of 135 K (243^{o} R).

Three 0.56-meter- (22-in.-) diameter aluminum spherical tanks having wall thicknesses of 0.056 centimeter (0.022 in.) were insulated with a 2.54-centimeter- (1.0-in.-) thick, rigid, freon-blown, polyurethane foam insulation having a nominal density of 32 kilograms per meter^{3} (2 lb/ft^{3}). The first two tanks were insulated using a foaming-in-place process with each tank suspended within a cylindrical mold. The third tank was insulated with a foam having a slightly different formulation using a simplified foaming-in-place process where the foam constituents were poured directly on the tank wall and allowed to expand in a radial direction.

Experimental testing conducted on the foam insulated tanks included (1) chilldown and boiloff tests to determine foam temperature profiles, thermal conductivity, and structural integrity under simulated ground-hold conditions, (2) vibratory compressive tests under simulated ground-hold and launch conditions, and (3) chilldown tests for simulated space-hold conditions where the entire foam thickness was chilled to temperatures near that of liquid hydrogen (21 K or 37^{o} R).

The initial foaming-in-place technique utilizing a cylindrical mold produced a foam insulation (1) where the direction of foam rise relative to the tank wall varied from the top to the bottom of the tank, and (2) that failed structurally under both ground-hold and space-hold test conditions. The simplified foaming-in-place technique in which the foam constituents were poured directly on the tank wall, coupled with the specific foam formulation, produced a foam insulation having (1) the direction of foam rise everywhere

normal to the tank wall, (2) relatively uniform cell size and structure, and (3) relatively small differences in the thermophysical properties parallel and perpendicular to the direction of foam rise. This foam insulation provided the desired thermal performance and remained structurally intact through all ground-hold, vibratory, and space-hold tests performed.

In addition, thermophysical properties of the polyurethane foam were obtained from the testing of small samples. These results were incorporated in an analytical program to predict the tangential and radial thermal stress profiles within the foam insulation created by imposing temperature gradients across the layer of foam typical of both ground-hold and space-hold conditions.

INTRODUCTION

Lightweight foam insulation has been proposed and/or utilized as a component of the insulation system for liquid hydrogen tanks of several booster or space vehicles. A layer of foam can be bonded directly on the inside of the tank wall (e.g., the Saturn S-IVB stage of ref. 1) or on the outside of the tank wall (e.g., the Saturn S-II stage of ref. 2). A proposed insulation system for the Centaur upper stage consisted of a layer of foam encased in an impermeable vapor barrier prior to bonding to the tank wall (ref. 3). For space vehicles requiring thermal protection for longer periods of time (greater than 6 hr), a sublayer of sealed foam bonded directly to the tank wall may be utilized in conjunction with a multilayer insulation purged with gaseous nitrogen under ground-hold conditions (ref. 4).

A problem area common to all insulation systems where a layer of foam was bonded directly to the outside of the liquid hydrogen tank was traced to the relatively large difference in the coefficients of thermal contraction between the foam and the metallic tank wall. The greater thermal contraction of the foam insulation generally caused it to crack or split when the tank was cooled down to liquid hydrogen temperature - approximately 21 K or 37° R (e.g., ref. 5). The cracking would, in turn, allow cryo-pumping of condensable purge gases within the foam and could cause structural degradation of the foam upon a subsequent warmup of the tank.

The type of foam generally proposed for use with liquid hydrogen tank insulation systems was a 32-kilogram-per-meter^3- (2-lb/ft^3-) density, closed-cell, rigid, freon-blown, polyurethane foam having a thermal conductivity of approximately 0.015 watt per meter per K (0.0087 Btu/(hr)(ft)($^{\circ}$R)) at a mean temperature of 135 K (243° R). However, because of problems with cracking or splitting, the foam normally had to be strengthened or reinforced by (1) increasing the foam density, (2) utilizing a plastic honeycomb, or (3) adding fiberglass or nylon threads either selectively or randomly

oriented in the foam. The use of any of these techniques of structurally reinforcing the foam necessarily increased both the weight and the thermal conductivity of the foam insulation, either of which is undesirable.

The objective of the investigation reported herein was to develop and test a 32-kilogram-per-meter^3- (2-lb/ft^3-) density polyurethane foam that would have the following properties:

(1) It could be foamed in place on the outside of a liquid hydrogen tank and be machined to the required thickness.

(2) It would not require any strengthening or reinforcing to prevent cracking or splitting.

(3) It would have a thermal conductivity of about 0.015 watt per meter per K (0.0087 Btu/(hr)(ft)($^\circ$R)) at a mean temperature of 135 K (243° R).

Several foam formulations were investigated and two were selected for further testing on the basis of compressive strength, flow properties, and cell uniformity. The foams were poured in place using two different techniques on spherical aluminum tanks having diameters of 0.56 meter (22 in.) and wall thicknesses of 0.056 centimeter (0.022 in.). Experimental tests conducted on the foam insulation included the following:

(1) Chilldown and boiloff tests under simulated "ground-hold" conditions to determine foam temperature profiles, thermal conductivity, and structural integrity of the foam

(2) Vibratory compressive tests under simulated ground-hold and launch conditions with peak loadings up to 21.2×10^4 newtons per meter^2 (30.8 lb/in.^{2}) at frequencies up to 30 hertz to again demonstrate structural integrity

(3) Chilldown tests for simulated space-hold conditions where the entire foam thickness was chilled to temperatures near that of liquid hydrogen (21 K or 37° R) to further demonstrate structural integrity - This simulates the conditions that might be imposed during space hold on a layer of foam utilized as a sublayer beneath a multilayer insulation system.

In addition, thermophysical properties of the polyurethane foam were obtained from the testing of small samples. These results were incorporated in an analytical program to predict the tangential and radial thermal stress profiles within the foam layer created by imposing temperature gradients across the layer of foam insulation typical of both ground-hold and space-hold conditions.

APPLICATION OF FOAM AND VAPOR BARRIER

A total of three thin-wall spherical tanks were fabricated from 6061 aluminum; each tank had a diameter of 0.56 meter (22.0 in.) and a wall thickness of 0.056 centimeter

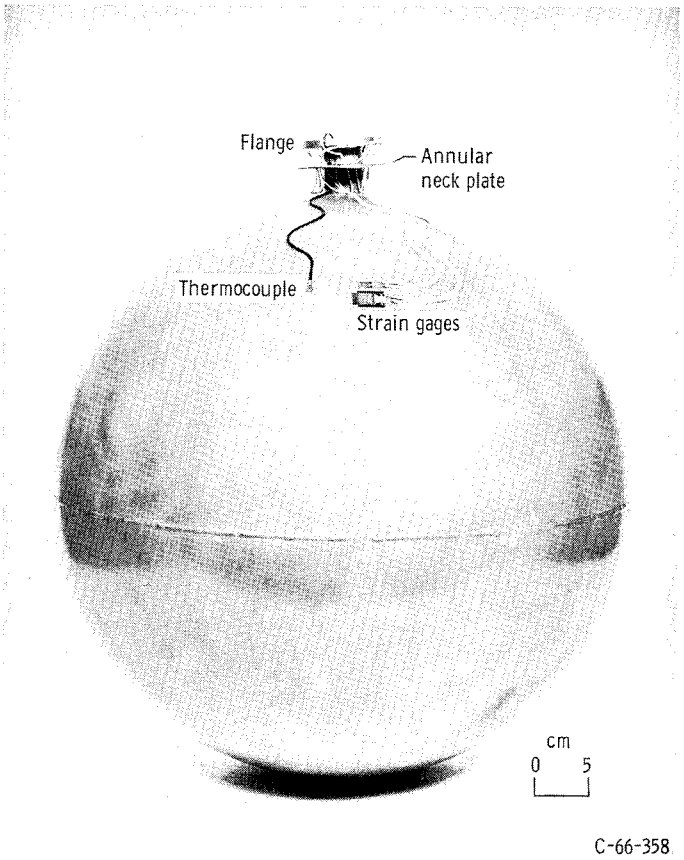

Figure 1. - Spherical aluminum test tank with 0.56-meter (22.0-in.) diameter.

(0.022 in.). Prior to the application of the foam insulation, each tank was primed with a 0.0025-centimeter (1-mil) thickness of Goodyear G-207 adhesive. Each tank was also instrumented with two copper-constantan thermocouples and four stabilized Armour D foil strain gages which were bonded to the outside of the tank (fig. 1).

Tanks 1 and 2

The first two spherical tanks were insulated in a like manner utilizing the foam formulation described in reference 3 and noted in table I. The foaming-in-place technique was as follows.

Upper half of tank. - The region around the neck between the annular neck plate and the tank wall was prefoamed and trimmed first. The tank was then mounted upside down within a cylindrical mold and held secure by means of a flange (fig. 2(a)). The lower half of the tank was masked off, and the tank and mold were preheated to 322 K (580^{o} R). The foam formulation was mixed and poured in liquid form directly into the mold. The foam was allowed to expand and set at 322 K (580^{o} R). The tank was then removed, and

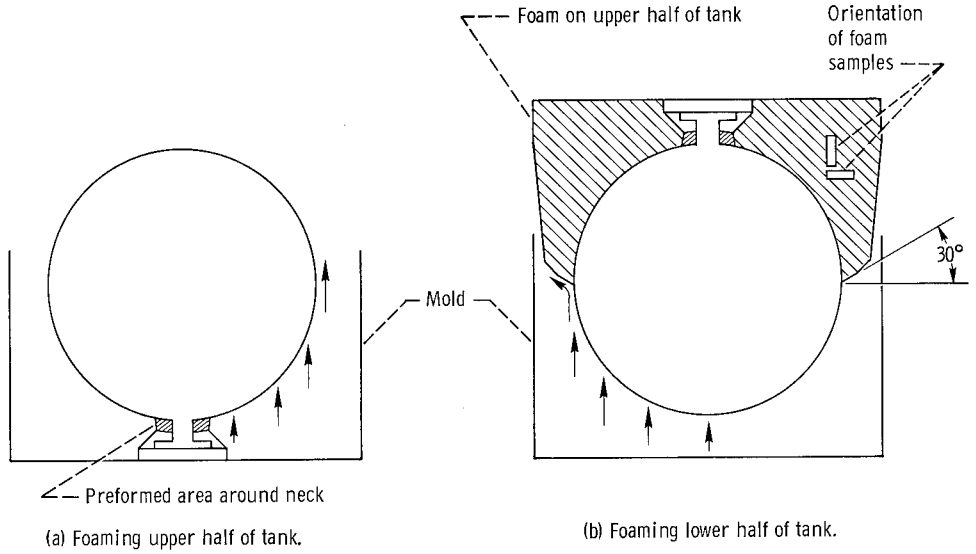

Figure 2. - Orientation of test tank in cylindrical mold for foaming upper and lower halves of tanks 1 and 2. (Arrows indicate direction of foam rise.)

the foam interface between the insulation on the upper and lower halves of the tank was arbitrarily machined with a 30^{o} angle between a normal to the tank wall at the equator and the surface of the interface (fig. 2(b)). The interface was not primed with any adhesive prior to applying the foam insulation on the lower half of the tank.

Lower half of tank. - The tank was suspended upright from above the cylindrical mold (fig. 2(b)). The foam was then applied to the lower half of the tank in the same manner as for the upper half.

The tank was then mounted in a vertical boring mill where the foam insulation was machined to a layer having a uniform thickness of 2.54±0.08 centimeters (1.0±0.03 in.). A vapor barrier was fabricated from a laminate of mylar and aluminum foil (mylar/aluminum/aluminum/mylar) composed of 0.00127/0.00076/0.00076/0.00127-centimeter (0.5/0.3/0.3/0.5-mil) layers. The laminate was stretch-formed and bonded to the outside of the foam layer utilizing a small number of gore panels. The lap joints between gore panels of the vapor barrier were additionally sealed with a laminate doubler strip. The completed tank is shown in figure 3. The average foam density for tank 1 was 29.4 kilograms per meter^3 (1.84 lb/ft^3); for tank 2, it was 32.0 kilograms per meter^3 (2.00 lb/ft^3).

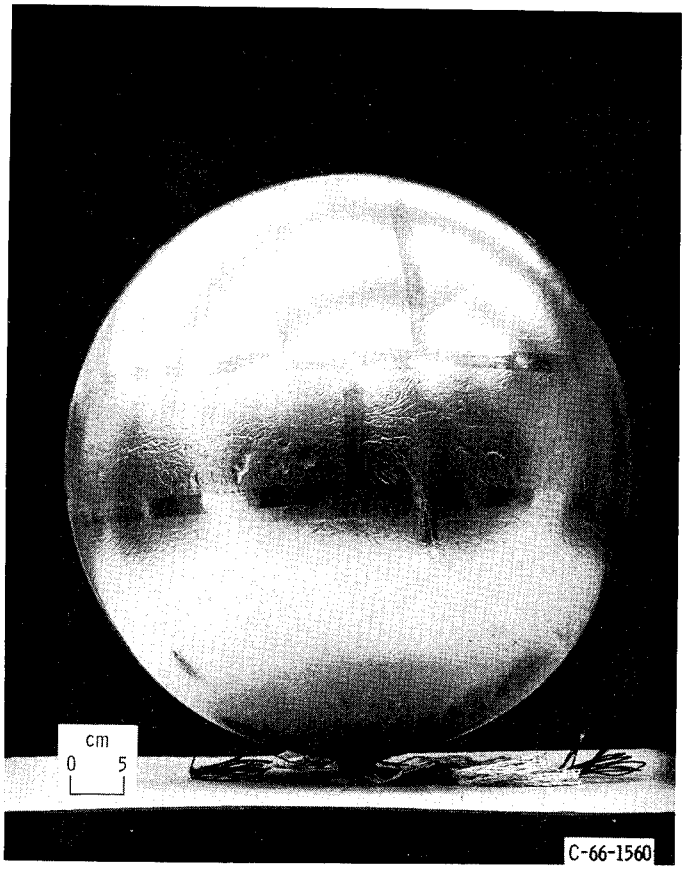

Figure 3. - Completed foam insulated tank - typical of tanks 1 and 2.

Tank 3

Based on the experimental test results for the first two tanks, the foam formulation for the third spherical tank was altered slightly to provide better flow properties, higher compressive strength, and more uniform cell structure; the constituents of the altered form formulation for tank 3 are noted in table I. The foaming-in-place technique was as follows.

Upper half of tank. - The area around the neck of the tank was again prefoamed, and the lower half of the tank was masked off. The tank was then preheated to 322 K (580° R). The foam formulation was mixed and poured in liquid form by hand directly on the upper half of the tank to uniformly wet the tank wall before the blowing action of the foam took place. The foam was allowed to expand radially and set at 322 K (580° R). The radial expansion of the foam was substantiated by noting the cellular structure of samples taken from preliminary pours on practice tanks. After cooling, the foam interface between the insulation on the upper and lower halves of the tank was machined. Foam interface angles (angle between the normal to the tank wall at the equator and the surface of the interface) of 30°, 45°, and 60° were investigated. The 30° angle was found to produce the best uniformity in cell structure of the foam applied on the lower half of the tank adjacent to the interface. The interface was not primed with any adhe-

sive prior to applying the foam insulation on the lower half of the tank.

Lower half of tank. - The outside surface of the previously applied foam insulation (except for the interface) was masked off and the tank was inverted. The foam insulation was then applied in the same manner as for the upper half of the tank.

The thickness of the radially expanded foam insulation obtained varied between 4 and $4\frac{1}{2}$ centimeters ($1\frac{1}{2}$ and $1\frac{3}{4}$ in.). Therefore, the tank was again placed in the vertical boring mill where the insulation was machined to a uniform thickness of 2.54±0.08 centimeters (1.0±0.03 in.). Prior to the application of the vapor barrier, a two-way stretch nylon fabric was bonded to the entire foam surface. The purpose of this fabric was to provide a bleeder ply to (1) vent any gas permeating or leaking through the vapor barrier to a vacuum/vent tube and (2) increase the radius of curvature of any wrinkles forming in the vapor barrier. The vapor barrier itself was fabricated in a manner identical to that of the first two insulated tanks described previously. A vacuum/vent tube was installed in the vapor barrier, and the vapor barrier was subsequently helium leak checked to ensure a relatively gas tight barrier. (A pressure less than 0.1 micron could be maintained behind the vapor barrier with no indication of a leak when the outside of the vapor barrier was sprayed with gaseous helium.) The completed tank is shown in figure 4. The average foam density was 34.4 kilograms per meter^3 (2.14 lb/ft^3).

Figure 4. - Completed foam insulated tank 3.

INSTRUMENTATION

Tanks 1 and 2

In addition to the two thermocouples and four Armour D foil strain gages mounted on the tank wall, the first two tanks were also instrumented with two patterns of five copper-constantan thermocouples (utilizing 0.0127-centimeter- (or 0.005-in.-diam. wire)), each embedded radially in the foam insulation, to determine its steady-state temperature profile (fig. 5). For these two tanks, no unusual care was taken to (1) provide good thermal contact between the thermcouple junctions and the foam insulation or (2) reduce

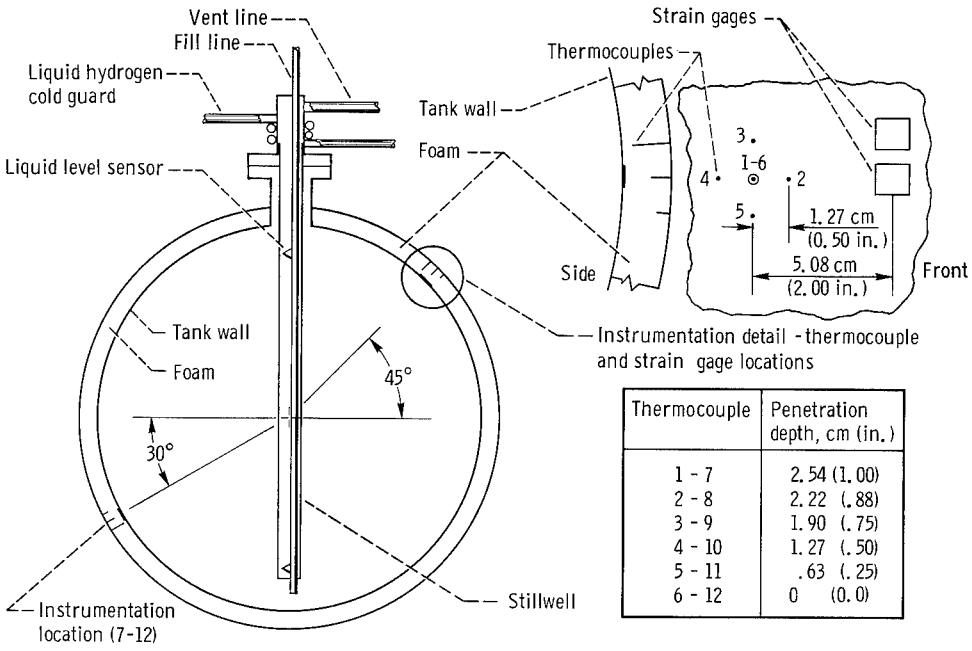

Thermocouple	Penetration depth, cm (in.)
1 - 7	2.54 (1.00)
2 - 8	2.22 (.88)
3 - 9	1.90 (.75)
4 - 10	1.27 (.50)
5 - 11	.63 (.25)
6 - 12	0 (0.0)

Figure 5. - Instrumentation details for tanks 1 and 2.

the heat leak through the electrical leads to the thermocouple junction. Also, two hot-wire liquid level sensors were mounted on the fill line within a Stillwell to provide indications of liquid level within the tank at the start and end of the boiloff tests.

Tank 3

Tank 3 was instrumented in the same manner as the first two tanks with the excep-

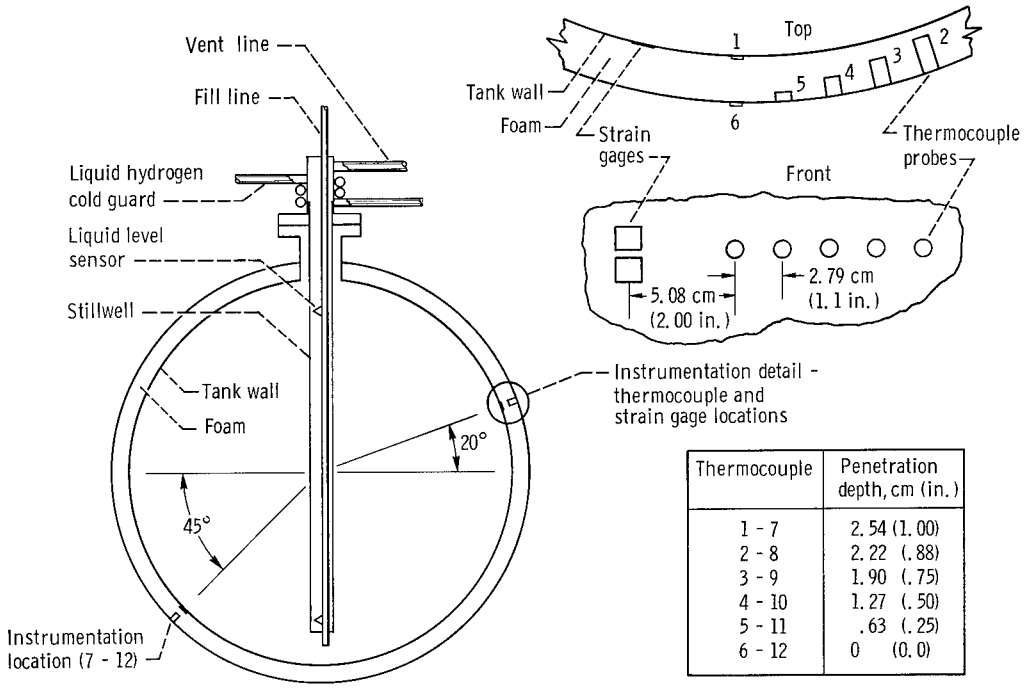

Thermocouple	Penetration depth, cm (in.)
1 - 7	2.54 (1.00)
2 - 8	2.22 (.88)
3 - 9	1.90 (.75)
4 - 10	1.27 (.50)
5 - 11	.63 (.25)
6 - 12	0 (0.0)

Figure 6. - Instrumentation details for tank 3.

tion of the thermocouple configuration and pattern (fig. 6). For the third tank, the thermocouple configuration was changed to (1) provide good contact between the thermocouple junction and the foam insulation and (2) reduce the heat leak through the electrical leads to the thermocouple junction. Each thermocouple (fig. 7) consisted of a 0.95-centimeter- (3/8-in. -) diameter by 0.025-centimeter- (0.01-in. -) thick copper disk which would (1) provide a large contact area with the foam and (2) act as the thermocouple junction. The 0.0127-centimeter (0.005-in. -) teflon insulated thermocouple wires were soldered to the copper disk to form the thermocouple junction. The thermocouple wires were then wound in a coil on a teflon mandrel at 19.7 turns per centimeter-wire to the desired thermocouple penetration depth. The wires were cemented together after which the teflon mandrel was withdrawn. When installed in the foam insulation, the copper disk and wire coil were cemented in a flat-bottom cylindrical hole drilled to the proper penetration depth in the foam. The interior of the wire coil was then filled with a cylindrical plug of foam which was cemented in place.

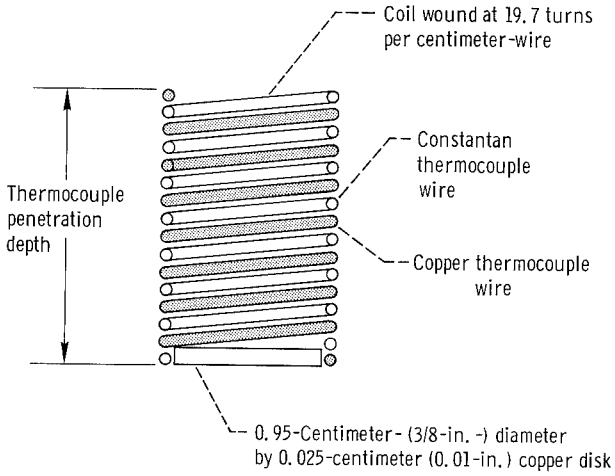

Figure 7. - Thermocouple configuration for tank 3.

A brief calibration of this thermocouple configuration was conducted using liquid nitrogen as the cold sink. The test thermocouple was mounted in a 10.2-centimeter (4.0-in.) square block of polyurethane foam along with a reference thermocouple and a surface thermocouple (fig. 8). The penetration depth of the test thermocouple was chosen such that it should indicate about the same temperature with the liquid nitrogen cold sink as the 2.22-centimeter- (0.88-in.-) penetration depth thermocouple (the thermocouple probe most deeply penetrating the foam insulation and indicating the lowest temperature) would on the foam insulated liquid hydrogen tank. The reference thermocouple consisted of a copper-disk thermocouple junction with more than 25.4 centimeters (10 in.) of wires spiral wrapped to provide a near-zero heat leak to the thermocouple junction. This type of thermocouple could not be utilized directly on the foam insulated tank because its large diameter (~2.5 cm or 1.0 in.) would require cutting a large hole in the foam insulation. During the calibration, the foam block was mounted in a liquid nitrogen Dewar such that the edge effects on the one-dimensional temperature profile in the block were minimized.

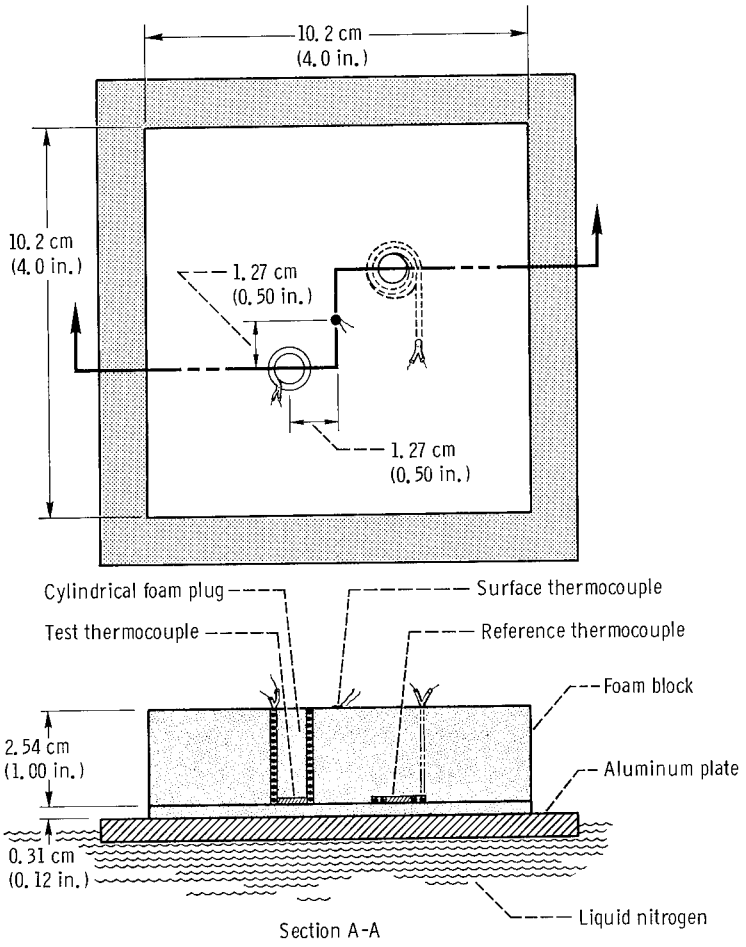

Figure 8. - Calibration apparatus for test thermocouple.

EXPERIMENTAL APPARATUS

Chilldown and Boiloff Tests

The chilldown and boiloff test apparatus was designed to simulate ground-hold tests of the foam insulation while also providing a means to (1) chill down the foam insulated tank at varying rates and (2) determine the thermal conductivity of the insulation by measuring the volumetric flow rate of the boiloff gas. The test apparatus is shown in figure 9.

The test tank was installed within a clear plastic box so that the insulation could be observed throughout a test. The box was purged with dry gaseous nitrogen to prevent

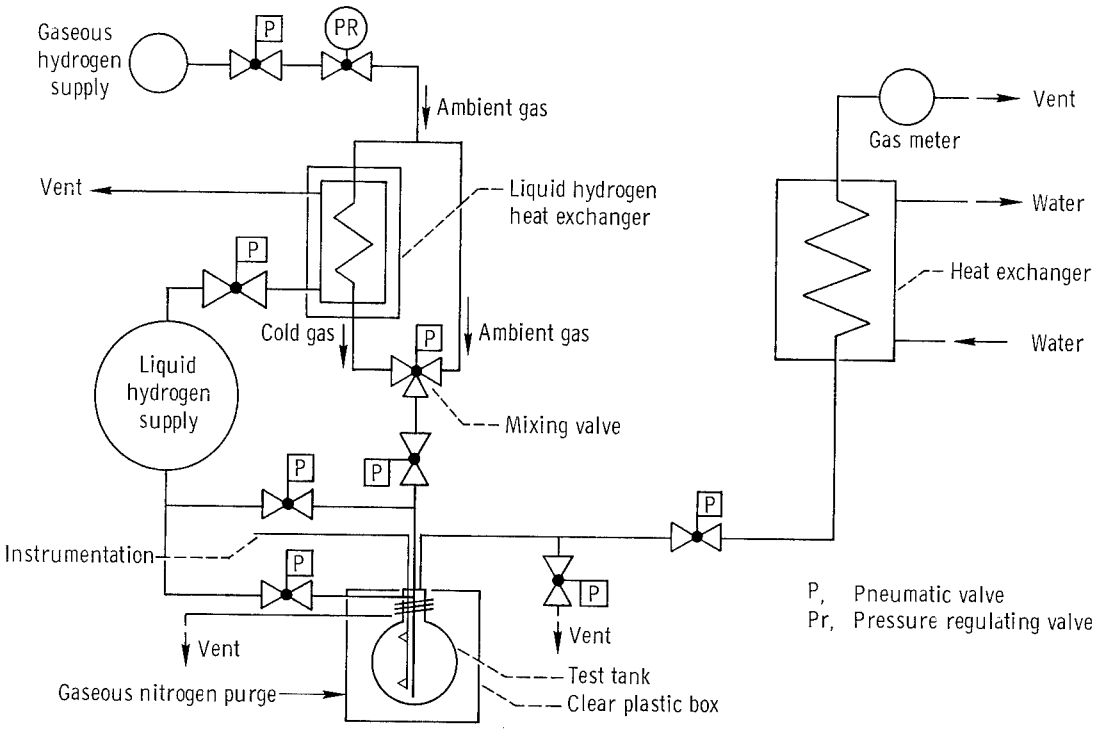

(a) Schematic view.

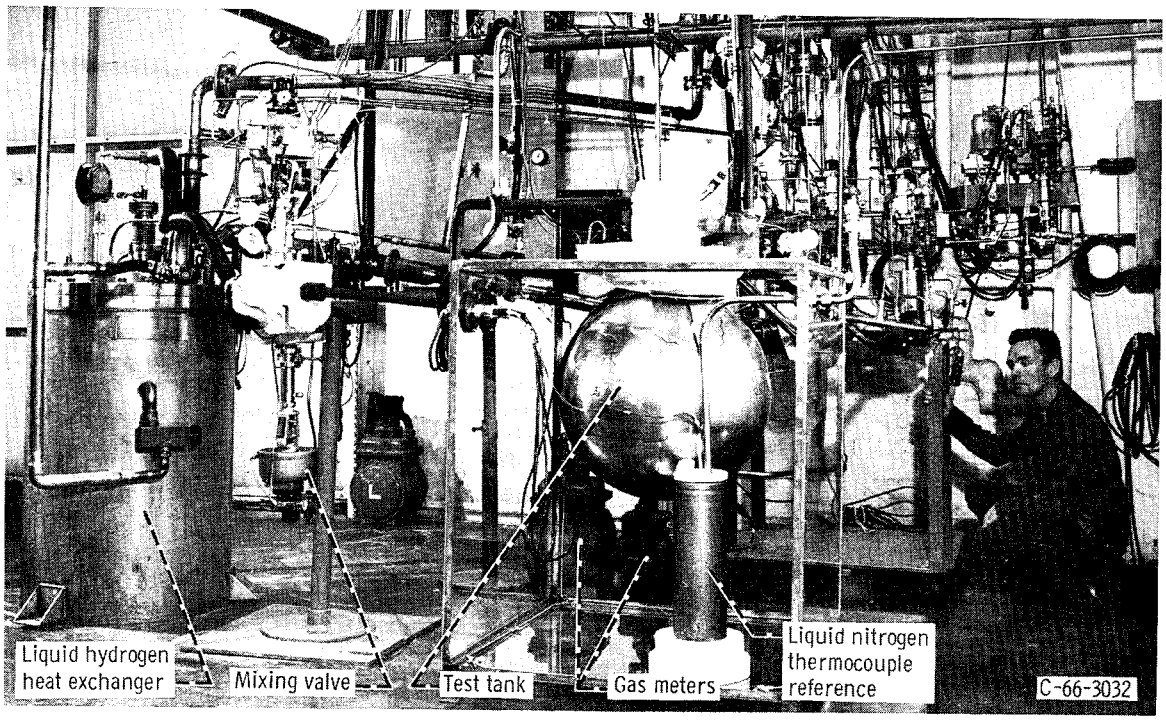

(b) Pictorial view.

Figure 9. - Variable chilldown rate and boiloff apparatus.

water vapor from freezing on the insulation. Gaseous hydrogen flowing into the test tank from an ambient temperature supply trailer could be cooled to any given temperature down to approximately 70 K (125° R) at the inlet to the tank. The gas temperature was controlled by a mixing valve which varied the relative amounts of gaseous hydrogen flowing through and bypassing a liquid hydrogen heat exchanger. The mixing valve could be operated in either a manual or automatic mode of operation. The chilldown rate of the foam insulated tank could then be controlled by manually adjusting the set point of the mixing valve controller. Once the tank was chilled down to 70 K (126° R), it was filled directly from a liquid hydrogen Dewar.

Once the temperature profile through the foam insulation had stabilized after a liquid hydrogen fill, the tank was topped off and then locked up except for the vent line. The boiloff gas was vented through a water heat exchanger and then through a dry gas meter having a usable range of 0 to 0.425 cubic meter per minute (0 to 15 scfm). A constant tank back-pressure controller was not needed during the boiloff tests because of the relatively large heat leak into the tank. The thermal conductivity of the foam insulation was then determined from the volumetric boiloff rate and the measured boundary temperatures of the insulation.

Vibration Apparatus

The vibration apparatus was designed to allow a vibratory compressive loading to be superimposed upon a static compressive loading of the foam insulation on the spherical tank. The compressive loads could be applied to the foam insulated tank either at ambient room temperature or when filled with liquid hydrogen.

The apparatus (fig. 10) consisted of the following:

(1) Annular-ring and circular tank supports having horizontal cross-sectional areas of 3.63×10^{-2} meter^2 (0.391 ft^2) between which the tank was mounted

(2) A strain-gage-type load cell to determine both vibratory and static compressive loads imposed upon the foam insulation

(3) A hydraulic cylinder and piston to provide static and vibratory loads up to 7680 newtons (1730 lb) at frequencies up to 30 hertz

(4) Steel frame and concrete block

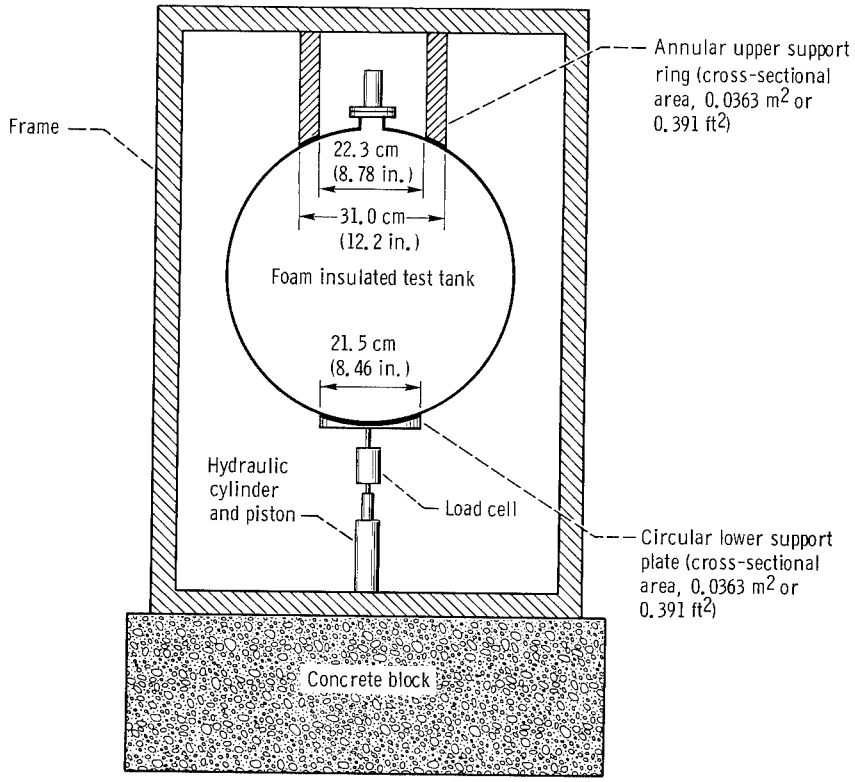

Figure 10. - Schematic view of vibration apparatus.

Space-Hold Apparatus

The space-hold environment tests were conducted in an existing cylindrical tank approximately 0.76 meter (30 in.) in diameter and $2\frac{1}{2}$ meters (8 ft) long that was converted to vacuum use. Pressures less than 1 micron could be maintained within the vacuum tank. For the more severe space-hold tests, the foam insulated tank was placed in a liquid hydrogen cooled shroud 0.71 meter (28 in.) in diameter and 0.76 meter (30 in.) long and/or insulated with aluminized mylar multilayer insulation to impose a low temperature throughout the foam insulation.

RESULTS AND DISCUSSION

Chilldown and Boiloff Tests, Tanks 1 and 2

Tank 1. - The first foam insulated tank was subjected to one chilldown and boiloff test as noted in table II. The tank was chilled down from ambient room temperature at the rate of 1.1 K per minute (2° R/min). During the chilldown, large depressions appeared in the foam insulation around the equator of the tank (fig. 11) causing severe wrinkling of the vapor barrier. These depressions resulted from the atmospheric pressure loading on the vapor barrier over an apparent structural failure of the foam. The subsequent boiloff test indicated a thermal conductivity for the foam insulation of 0.015 watt per meter per K (0.0087 Btu/(hr)(ft)($^{\circ}$R)) at a mean temperature of 147 K

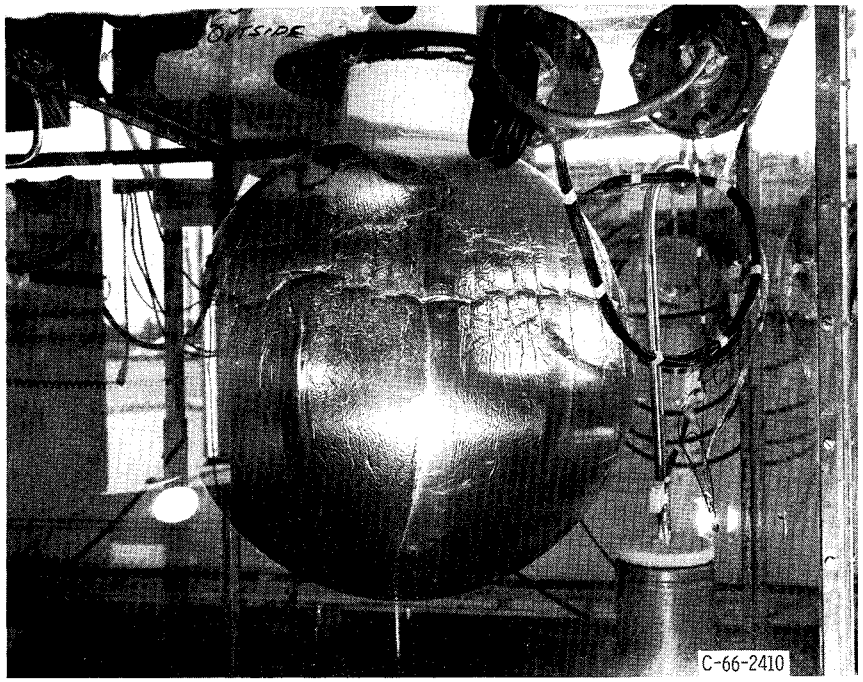

Figure 11. - Indentation in foam during chilldown and liquid hydrogen fill (tank 1.)

(264° R) which met the original specifications. For this test, the average measured temperature of the outside of the tank wall was approximately 28 K (50° R). The wrinkles formed in the vapor barrier while the tank was filled with liquid hydrogen created small leaks which allowed the nitrogen purge gas to penetrate behind the vapor barrier in several areas near the equator of the tank. During the warmup of the tank to ambient room temperature, the nitrogen gas expanded and created several large blisters in the vapor barrier. A period of several hours was required before the gas pressure forming

the blisters was reduced to 1 atmosphere absolute pressure. The large depression in the foam, however, had largely disappeared immediately after the warmup was completed. The vapor barrier was subsequently stripped from the foam insulation near the equator of the tank; however, no cracks or other evidence of structural failure were noted on the surface of the foam. Subsequent cuts into the foam insulation revealed large voids in the foam adjacent to the tank wall (fig. 12). These voids extended completely around the tank just below the equator. In addition, many small voids were also noted in the foam adjacent to the foam interface on the lower half of the tank. All of the voids were apparently created during the application of the insulation to the lower half of the tank where the foam (1) had a direction of rise parallel to the tank wall and (2) had to change direction of flow at the foam interface (fig. 2(b)).

Tank 2. - A total of five chilldown tests of varying rates and four boiloff tests were conducted on the second spherical tank (table II). During all five chilldown tests, depressions in the foam around the equator of the tank were again noted. These depressions again caused wrinkles in the vapor barrier which created leaks. During each warmup, the gas (which had leaked through) expanded and created blisters in the vapor barrier which became progressively worse with each test. At the end of test 4, the

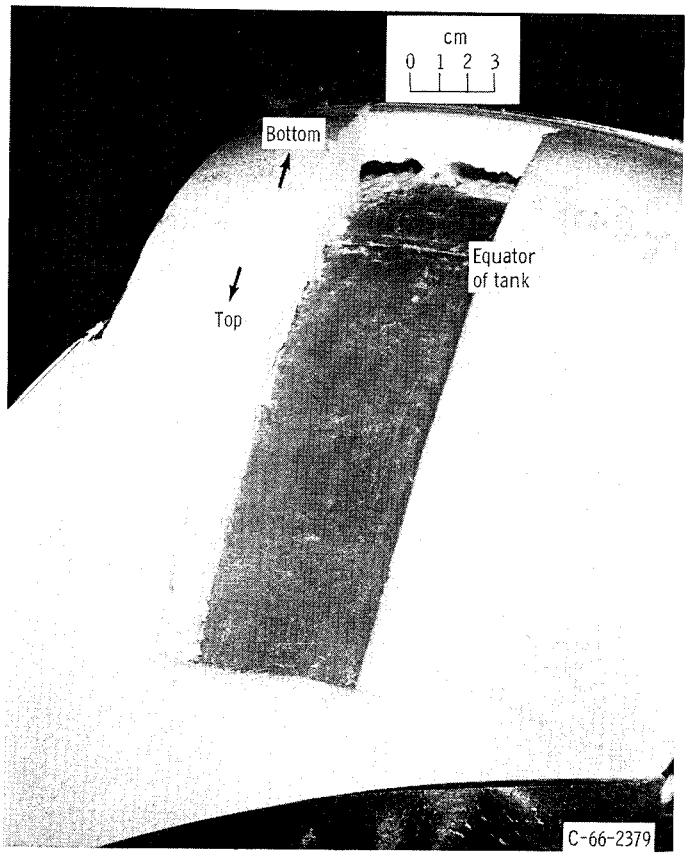

Figure 12. - Typical voids in foam insulation adjacent to tank wall (tank 1).

mylar-laminate vapor barrier was completely removed, and the outside surface of the foam was painted with several thin coats of G-207 adhesive. No damage or structural degradation of the G-207 adhesive was noted after ground-hold test 5.

The measured values of thermal conductivity averaged to 0.0146 watt per meter per K (0.0085 Btu/(hr)(ft)(^{o}R)) at a mean temperature of 150 K (270^{o} R); no measurable degradation of thermal performance due to (1) increased chilldown rate or (2) thermal cycling was noted during the tests.

Inspection of the foam insulation after all tests were completed again revealed numerous voids adjacent to the tank wall around the equator or the tank similar to those noted previously for tank 1.

Space-Hold Test, Tank 2

Two simulated space-hold tests of the second foam insulated tank were conducted. For the first test, neither aluminized mylar insulation nor the liquid hydrogen cooled shroud were utilized. The G-207 adhesive coating apparently provided a high emissivity outer surface, and the foam surface temperature was reduced to only 234 K (421^{o} R). The foam insulation survived intact.

For the second test, multilayer insulation consisting of six layers of single-aluminized mylar was applied over the foam insulation to reduce the radiation heat transfer to the tank. The final foam surface temperature achieved during this test is not known since the foam insulation cracked and severely strained or severed all thermocouple leads. A post-test inspection revealed numerous hairline cracks in the G-207 adhesive coating as well as at the surface of the foam in the middle half of the tank centering about the equator. Because of the damage to the foam insulation, no further tests (space hold or vibration) were conducted.

Foam Insulation Improvements, Tank 3

The polyurethane foam formulation and technique of application were changed for the third spherical tank in an effort to overcome problem areas noted during tests of the first two foam insulated tanks. These problem areas and potential solutions are noted as follows.

Elimination of voids adjacent to tank wall. - The method of application of the foam on the tank was changed to allow the constituents of the foam formulation to be poured directly onto one-half of the tank at a time. More than two dozen tests conducted utilizing four different foam formulations, wherein the foam constituents were poured directly on

rubber balloons of about the same size as the aluminum tanks, indicated that (1) the tank wall could be uniformly wetted by the constituents and (2) the resulting layer of foam was of relatively uniform cell size and structure and contained no voids within the layer. The specific foam formulation chosen for tank 3 (table I) possessed the highest compressive strength normal to the tank wall based on room temperature tests.

Elimination of voids adjacent to split line. - Tests were conducted wherein the foam interface angle at the equator of the tank between the insulation applied to the upper and lower halves of the tank was varied (30°, 45°, and 60°). The 30° interface angle, combined with the new application technique and slightly improved flow properties of the foam formulation, produced only slight irregularities in the cell size or structure in the foam layer applied to the lower half of the tank adjacent to the split line.

Elimination of leaks in vapor barrier. - It was anticipated that the elimination of (1) voids within the foam and (2) irregularities in the surface of the foam (more uniform cell size and structure) would remove the cause of the wrinkles in the vapor barrier which ultimately created the gas leakage for the first two tanks. In the event that this problem did recur, however, a two-way stretch nylon cloth was bonded to the foam layer underneath the vapor barrier on tank 3 and a vacuum/vent tube was installed on the vapor barrier (fig. 4). The nylon cloth "bleeder ply" allowed any gas trapped underneath the vapor barrier to be vented around the tank to the vacuum/vent tap. The vapor barrier was helium leak checked after fabrication to ensure that all leaks were sealed. (A pressure less than 0.1 micron could be maintained behind the vapor barrier with no indication of a leak when the outside of the vapor barrier was sprayed with gaseous helium.) During thermal tests, the vacuum/vent tube would normally be sealed. However, if leaks did develop in the vapor barrier, the gas could be vented during the warmup of the tank. Or, alternately, the space beneath the vapor barrier could be pumped on with a vacuum pump during a thermal test.

Improvement in measurement of foam insulation temperature profiles. - During the chilldown and boiloff tests conducted on the first two tanks, it was noted that the measured temperatures within the foam insulation were considerably higher than anticipated. This was caused by the method of installation of the thermocouples. Since it was undesirable to use a large diameter plug in order to install the thermocouple lead wires isothermally within the foam insulation, a new thermocouple configuration shown in figure 7 was utilized. This thermocouple configuration provided (1) a large contact area with the foam insulation and (2) potentially low heat leaks through the thermocouple leads, both of which were deficiencies in the thermocouple installation on the first two tanks. In addition, this thermocouple configuration could still be installed within the foam layer without thermally or structurally degrading a large area of the foam insulation.

A calibration test of the new thermocouple configuration was conducted with liquid nitrogen utilizing the test configuration shown in figure 8. The average foam tempera-

tures measured over a 1/2-hour period of steady-state operation during this calibration were as follows: (1) surface temperature: 273.2 K (491.8° R), (2) test thermocouple: 116.3 K (209.3° R), and (3) reference thermocouple: 107.1 K (192.8° R). None of the measured temperatures varied by more than ±1.7 K (±3° R) during the half hour period. The temperature measured by the test thermocouple configuration T_m was then corrected to agree with that measured by the reference thermocouple by means of the following equation (Symbols are defined in appendix A.):

$$T_c = T_m - \left(\frac{g}{g_T}\right)(T_s - T_m) \tag{1}$$

where g is the required thermal resistance between the thermocouple junction disk and the foam insulation necessary to make the temperature correction and g_T is the thermal resistance of the thermocouple wires. If it is assumed that the value of g remains constant and that the value of g_T is dependent only upon the length of the thermcouple wires, then the resistance ratios g/g_T can be easily calculated for thermcouples having any given penetration depth. This assumption is generally valid since the thermal conductivity of both the copper and constantan thermocouple wires varies only slightly for temperatures above 111 K (200° R). The values of the resistance ratio used for this investigation are noted in table III.

Chilldown and Boiloff Tests, Tank 3

The third foam insulated tank was subjected to three chilldown tests of varying rates and three boiloff tests as noted in table II. The corrected measured-temperature profiles through the foam insulation on the top and bottom halves of the tank are shown in figure 13 for test 1. The tank wall was chilled down at the rate of 2.23 K per minute (4.01° R/min) which was followed by a 78-minute hold period to ensure that the temperature profile through the foam insulation had reached steady state. A boiloff test in which the volumetric boiloff rate was measured to determine the thermal conductivity of the foam insulation then followed. The large temperature difference of the tank wall between the top and bottom of the tank during the latter part of the boiloff test indicated that the boiloff rate would be a function of liquid level in the tank (as was expected and noted for all boiloff tests).

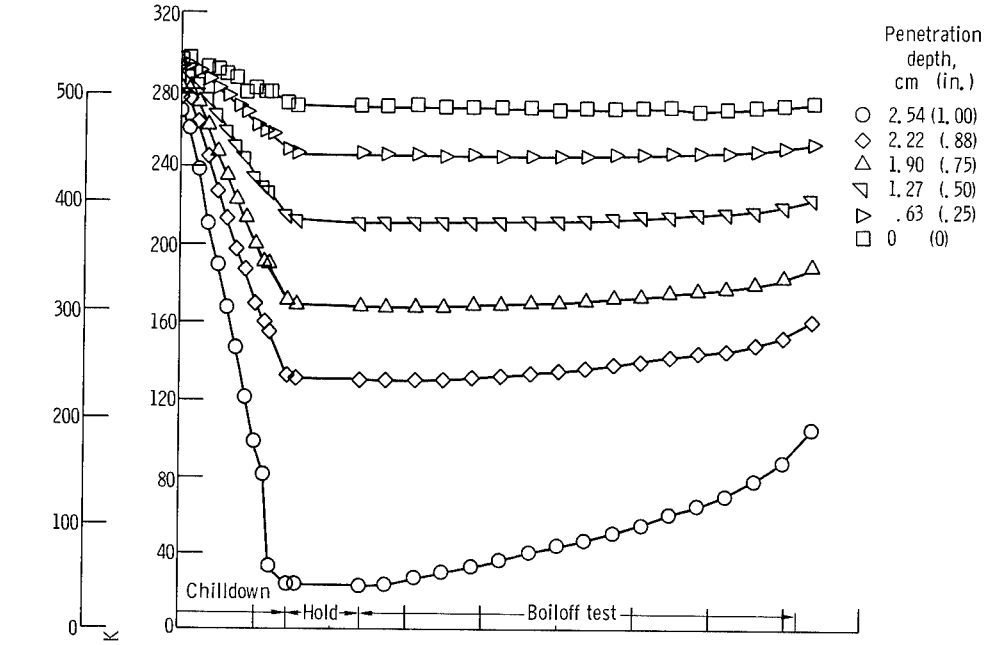

(a) Thermocouple pattern on upper half of tank.

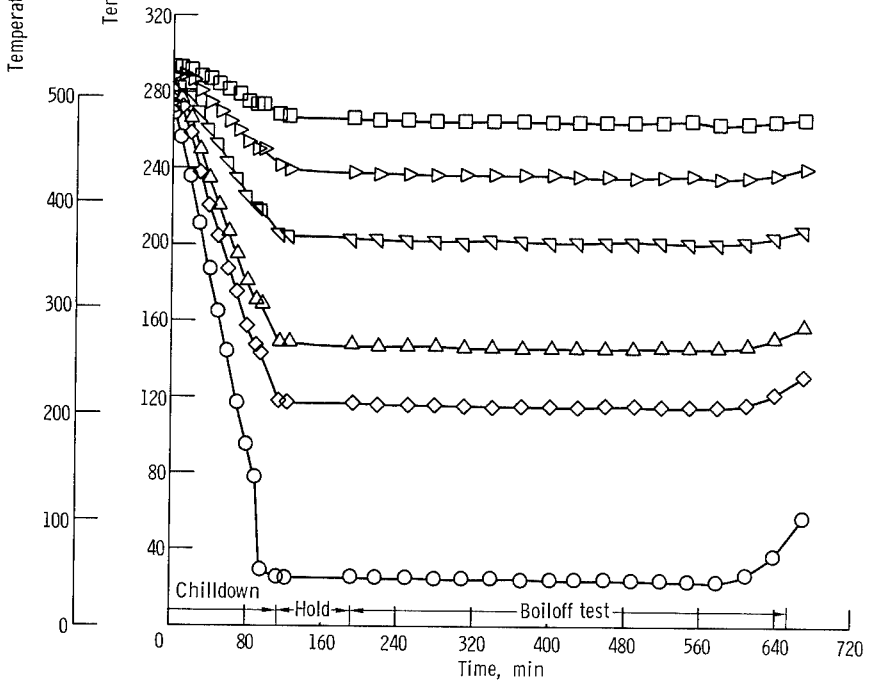

(b) Thermocouple pattern on lower half of tank.

Figure 13. - Foam insulation temperature profile for chilldown and boiloff test (tank 3, test 1).

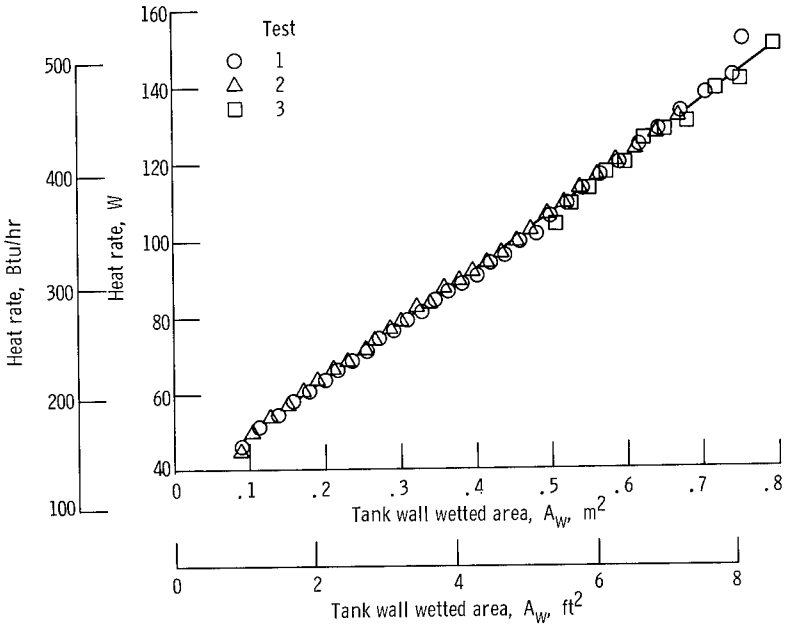

Figure 14. - Boiloff test results for tank 3.

The boiloff test results for tank 3 (which are typical of all boiloff tests conducted) are shown in figure 14 where the boiloff rate has been converted to the resultant total heat input and plotted as a function of the wetted tank wall area. The effective thermal conductivity of a given layer of foam insulation is then determined from the heat conduction equation (ref. 3) for a spherical shell

$$K = \left(\frac{\Delta Q}{\Delta A}\right)\left[\frac{t}{(T_S - T_W)}\right] \qquad (2)$$

where $\Delta Q/\Delta A$ is determined from the slope of the boiloff curve and adjusted to correspond to the mean area of the layer of foam insulation being considered. For application to a real system (i.e., when calculating the heat leak into an actual flight-weight liquid hydrogen tank under relatively high heat flux (ground-hold) conditions), only the area of the tank wetted by the propellant should be used.

The values of thermal conductivity of the foam insulation obtained from the boiloff tests of tank 3 (as well as the first two tanks) are shown in figure 15 (and also table II) and compared with values given in previously published literature (private communication from E. I. duPont de Nemours & Co. and refs. 6 and 7). The average overall thermal conductivity for tank 3 was 0.0137 watt per meter per K (0.0079 Btu/(hr)(ft)(^{o}R)) at a mean temperature of 135 K (243^{o} R) which again was better than the original specifications. Values of thermal conductivity as a function of mean temperature were also

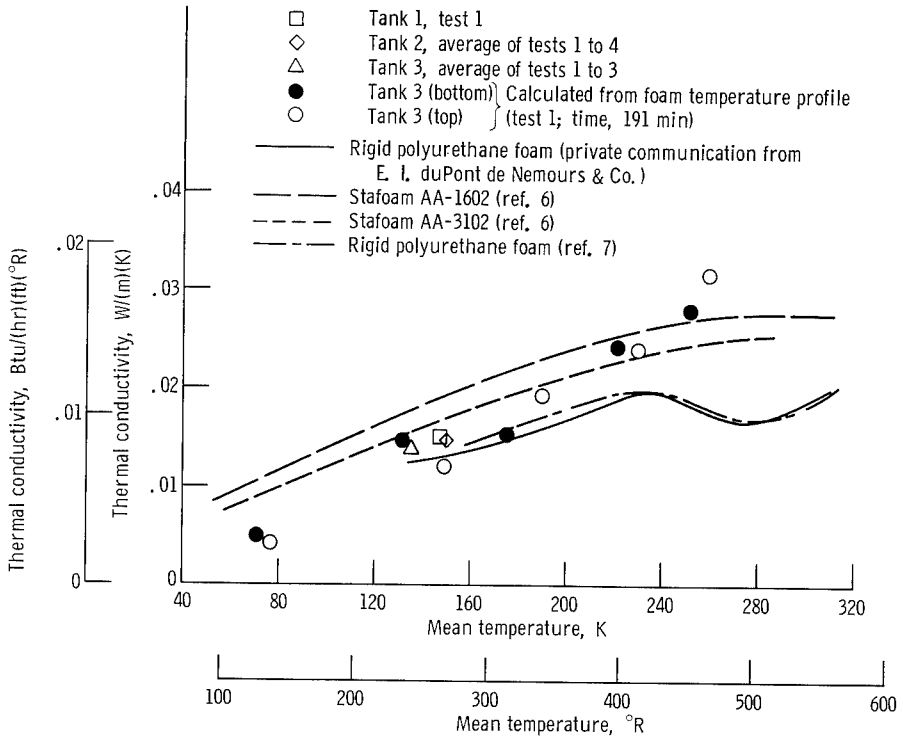

Figure 15. - Thermal conductivity of rigid polyurethane foam insulation.

calculated from the foam insulation temperature profiles for tank 3, test 1 at the start of the boiloff test (test time - 191 min). The experimentally determined values of thermal conductivity generally agree quite well with previously published data.

Only a very slight depression in the foam located at the foam interface around the equator of the tank was noted during tests 1 to 3 for tank 3. Even this slight depression could have been prevented by backing up the vapor barrier with a heavier strip of mylar film in the vicinity of the interface. No other structural degradation of any kind could be attributed to the thermal cycling. During each of the first three tests, the underside of the vapor barrier was (1) partially evacuated prior to the chilldown test and (2) vented to the atmosphere during the latter part of the warmup after completion of the boiloff test to prevent any possible blistering of the vapor barrier.

Vibration Tests, Tank 3

Vibration tests were conducted with the third spherical tank to further demonstrate the structural integrity of the foam insulation and also to simulate a possible space vehicle configuration where the support loads for the liquid hydrogen tank would be trans-

mitted entirely through the foam insulation without any other means of tank support. The tests were conducted with the tank pressurized to about 2.4×10^5-newtons-per-meter^2-gage (35-psig) pressure at both ambient room temperature and with the tank filled with liquid hydrogen. During the test, the tank was first statically loaded to approximately 1.03×10^5 newtons per meter^2 (15 psi) over the area of the support plates to simulate the launch vehicle boost loading. Then various vibratory loads at frequencies from 4.97 to 30.56 hertz were superimposed upon the static load (fig. 16) to simulate, to some degree, the vibrational loadings which might be present in the launch vehicle during the boost

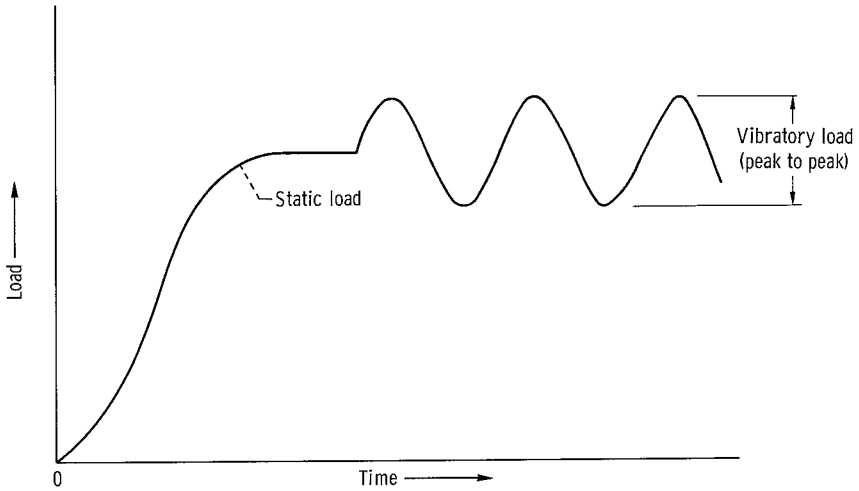

Figure 16. - Loading of foam insulated tank for vibration tests.

phase of the flight. The total test time under vibratory loads was 17.8 minutes at ambient temperature and 14.8 minutes when the tank was filled with liquid hydrogen. The test conditions are noted in table IV.

No cracking or structural degradation occurred to the foam during this period of testing except for the final static deflection (or set) in the foam around the bottom of the tank above the circular support plate (table IV). The final static deflection of 0.312 centimeter (0.123 in.) noted immediately after the tests were completed probably would have been smaller if the vibratory loadings had not inadvertently been increased far above the desired value of 1.03×10^5 newtons per meter^2 (15 psi) three times during the test. The deflection, however, had largely disappeared by the day following the warmup of the tank. No depression or set in the foam on the top of the tank under the annular support ring was observed at any time.

From these preliminary tests, it appears that a foam insulation would be capable of supporting a liquid hydrogen tank in this manner during booster launch conditions.

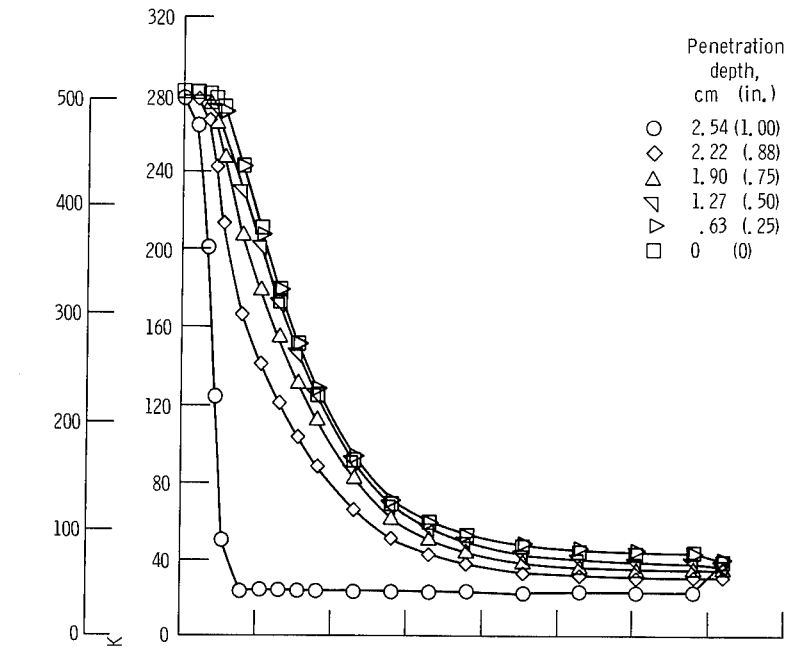

(a) Thermocouple pattern on upper half of tank.

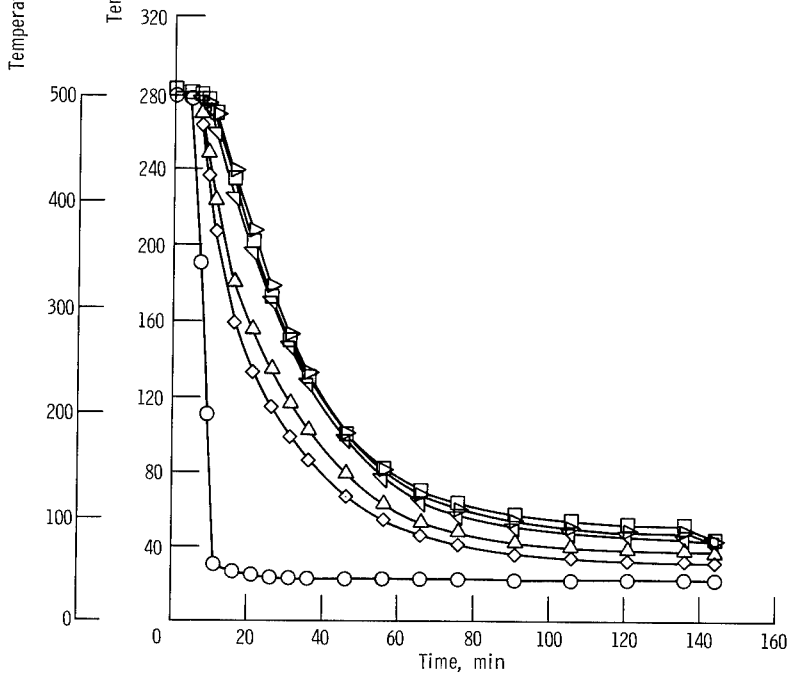

(b) Thermocouple pattern on lower half of tank.

Figure 17. - Foam insulation temperature profile for space-hold test (tank 3, test 7).

Space-Hold Tests, Tank 3

The third foam insulated tank was subjected to three simulated space-hold tests of increasing severity (decreasing surface temperature) as noted in table II. The foam insulation temperature profile for test 7 (the final test) is shown in figure 17. The temperature varied from 24 to 44 K (43° to 79° R) on the upper half of the tank and 23 to 53 K (41° to 95° R) on the lower half of the tank near the end of the test (the variation in temperature profiles is due to the circulation pattern of the hydrogen in the shroud). Subsequent stripping of the vapor barrier and visual inspection of the foam indicated no cracks, voids, or other structural degradation of the foam insulation due to the space-hold test or any of the previous tests except for the foam at the bottom of the tank which felt slightly "spongy" (a result of the vibration test).

If this foam insulation had been used on a liquid hydrogen tank as a sublayer underneath a nitrogen purged multilayer insulation, for example, it would have remained structurally intact and would have withstood the repeated thermal cycles under ground-hold and space-hold conditions that would be necessary during thermal tests and evaluation of the insulation system.

Foam Sample Testing

Foam samples obtained for each of the three spherical tanks were used to determine the following thermophysical properties (appendix B):

(1) Compressive yield strength and modulus of elasticity

(2) Tensile yield strength and modulus of elasticity

(3) Shear modulus of elasticity

(4) Thermal contraction

The results indicated that the thermophysical properties of the foam insulation on tank 3 tended to be more uniform between the orientations parallel and perpendicular to the direction of foam rise when compared to that for the first two tanks. This trend, coupled with the foaming-in-place technique, is believed to be responsible for the improved structural integrity of the foam insulation on tank 3 throughout all of the experimental testing.

Predicted Thermal Stress Profiles Within the Foam Insulation

The radial and tangential thermal stress profiles in the layer of foam insulation were calculated using the equations presented in reference 8 for concentric spherical shells

(appendix C). Stress profiles were calculated utilizing the foam properties and temperature profiles (tests 1 and 7) obtained for tank 3. In addition, stress profiles were calculated for a single generalized temperature profile imposed on foam insulation layers of varying thickness on an assumed 3.05-meter- (10-ft-) diameter tank to indicate the effect of tank size and insulation thickness.

The results indicated that the stresses were generally more severe for space-hold conditions than for ground-hold conditions, but that the stresses were well below the yield strength noted in the foam sample tests in all cases. In addition, the results indicated the following, for the same generalized temperature profile:

(1) The stress profiles are the same for different sized tanks having the same foam thickness to tank diameter ratios t/D.

(2) The radial stress profile decreased as the t/D ratio decreased.

(3) The tangential stress profile increased slightly as the t/D ratio decreased.

The strain gages mounted on the tank wall were to have been used in an attempt to measure the radial compressive stress at the tank wall-foam interface. In order to do this, the strain gages were carefully calibrated prior to the foam application to obtain the gage factor and calibration curves of apparent thermal strain (ref. 9). However, the resulting radial compressive stresses were so small that they could not be measured with sufficient accuracy; therefore, these results are not presented in this report.

SUMMARY OF RESULTS

Three thin wall, 0.56-meter- (22-in.-) diameter aluminum spherical tanks were insulated with 2.54-centimeter- (1.0-in.-) thick, rigid, freon-blown, polyurethane foam insulation and tested utilizing liquid hydrogen as the cryogenic test fluid. The first two tanks were insulated using a foaming-in-place process with each tank suspended within a cylindrical mold. The third tank was insulated with a slightly different foam formulation using a simple foaming-in-place process where the foam constituents were poured directly on the tank wall and allowed to expand in a radial direction. Experimental tests conducted included simulated ground-hold, vibration loading, and space-hold tests to determine the thermal performance and structural integrity of the foam insulation. In addition, small foam samples were tested to determine thermophysical properties. The test results may be summarized as follows:

1. The foaming-in-place technique (tanks 1 and 2) utilizing a cylindrical mold produced a foam insulation having many large voids at the tank wall-foam interface near the equator of the tank. These voids, occurring within the insulation applied to the second (lower) half of the tank, were apparently created during the application of the insulation where the foam (1) had a direction of rise parallel to the tank wall and (2) had to change

direction of flow at the foam interface. In addition, this foaming-in-place technique, coupled with the specific foam formulation, produced a foam having relatively large differences in the thermophysical properties parallel and perpendicular to the direction of foam rise. While this method of insulating liquid hydrogen was adequate for ground-hold testing using just foam insulation (even with the voids in the foam adjacent to the tank wall), the foam cracked during a simulated space-hold test and might not have been adequate for a ground-hold test where the foam was used as a sublayer beneath a nitrogen purged multilayer insulation.

2. The foaming-in-place technique (tank 3) in which the foam constituents were poured directly onto the tank produced a foam insulation having relatively good uniformity and with the direction of foam rise everywhere normal to the tank wall. This foaming-in-place technique, coupled with the specific foam formulation, produced a foam having relatively small differences in thermophysical properties parallel and perpendicular to the direction of foam rise. The foam remained structurally intact through all ground-hold, vibration, and space-hold tests.

3. The measured overall thermal conductivity of the foam insulation varied between 0.0137 and 0.0165 watt per meter per K (0.0079 and 0.0095 Btu/(hr)(ft)(^{o}R)) for mean temperatures of 135^{o} to 150^{o} R (243 to 270 K). Experimentally determined values of thermal conductivity as a function of temperature showed good agreement with previously published data.

4. The structural integrity of the foam insulation was not affected by the chilldown rate over a range of 1.1 to 47.0 K per minute (2.0^{o} to 84.6^{o} R/min) during a liquid hydrogen fill.

5. The foam insulation had sufficient strength to support a liquid hydrogen tank under simulated booster launch conditions (maximum compressive loadings of 2.12×10^{5} N/m^{2} or 30.8 psi) and vibratory frequencies up to 30 hertz when tank was at ambient room temperature or when filled with liquid hydrogen.

6. Since a mylar-aluminum laminate vapor barrier is prone to develop leaks where wrinkles may be formed at irregularities in the foam surface, the use of a nylon-backed, vented vapor barrier is desirable to prevent blisters from forming during warmup after repeated liquid hydrogen fills and/or test cycles. In addition, the use of a heavy mylar strip under the vapor barrier over known or expected locations of surface irregularities in the foam would help to prevent wrinkles from forming in the vapor barrier.

7. When isothermal thermocouple leads cannot be utilized in the measurement of foam insulation temperature profiles, the use of small diameter leads wrapped in a coil in conjunction with a disk-type thermocouple junction to the foam generally appears to be adequate if initially calibrated with a reference.

8. Thermophysical properties of the rigid polyurethane foam were obtained from tests conducted on small samples. The variations of compressive yield strength and

modulus of elasticity, tensile yield strength and modulus of elasticity, shear modulus of elasticity, and thermal contraction generally compared favorably with results obtained earlier. The fact that the foam insulation for tank 3 remained structurally intact throughout the thermal tests is believed to be due primarily to the combination of (1) the relatively small difference in thermophysical properties (particularly thermal contraction) parallel and perpendicular to the direction of foam rise and (2) the foaming-in-place technique.

9. Prediction of the foam radial and tangential stress profiles for varying temperature profiles encountered during ground-hold and space-hold conditions indicated that the thermal stresses were well below the yield strength of the foam at all times. Values of radial and tangential stresses for a given generalized temperature profile were determined to be independent of tank size for a given value of foam insulation thickness to tank diameter ratio. Decreases in the foam thickness to tank diameter ratio, for the same generalized temperature profile, indicated that (1) the radial compressives stresses also decreased and (2) the tangential tensile stresses increased very slightly.

Lewis Research Center,
National Aeronautics and Space Administration,
Cleveland, Ohio, November 7, 1968,
180-31-08-06-22.

APPENDIX A

SYMBOLS

A	mean area of concentric layer, $4\pi R_n R_{n+1}$, m^2; ft^2
A_w	wetted tank wall area, m^2; ft^2
E	modulus of elasticity, N/m^2; psi
g	thermal resistance of glue joint between thermocouple disk junction and foam insulation, K/W; (hr)(^oR)/Btu
g_T	thermal resistance of thermcouple leads, K/W; (hr)(^oR)/Btu
K	thermal conductivity, W/(m)(K); Btu/(hr)(ft)(^oR)
L	length of foam sample, cm; in.
N	number of concentric layers plus 1
n	concentric layer (n = 1, 2, 3, . . .)
P	interface pressure between two adjacent concentric layers, N/m^2; psi
Q	heat input rate, W; Btu/hr
R	radius of surface of concentric layer, m; ft
r	mean radius of concentric layer, m; ft
T	temperature, K; ^oR
T_c	corrected temperature of foam insulation, K; ^oR
T_m	measured temperature of foam insulation, K; ^oR
T_r	strain free reference temperature of foam insulation, K; ^oR
T_s	surface temperature of foam insulation, K; ^oR
T_w	temperature of tank wall, K; ^oR
t	thickness of foam insulation, m; ft
x	distance from tank wall, m; ft
W, X, Y, Z	constants
α	coefficient of thermal contraction, m/(m)(K); in./(in.)(^oR)
σ_r	radial stress, N/m^2; psi
σ_θ	tangential stress, N/m^2; psi
ν	Poisson's ratio

APPENDIX B

FOAM SAMPLE TESTS

For the first two spherical tanks, foam samples were taken from the excess foam cut away from the top and bottom halves of the insulation approximately 45^{o} above and below the equator of the tanks. The samples, oriented both parallel and perpendicular to the direction of foam rise (fig. 2(b)), were approximately 2.5 by 2.5 by 7.6 centimeters (1 by 1 by 3 in.) in size.

The foam samples for tank 3 were taken from a spare 0.56-meter- (22-in.-) diameter tank that was foamed at the same time as the test tank under the same conditions. The size of the foam samples obtained depended upon the sample orientation to the direction of foam rise; that is,

(1) 2.5- by 2.5- by 2.5-centimeter- (1- by 1- by 1-in.-) samples for orientations parallel to the direction of foam rise

(2) 2.5- by 2.5- by 7.6-centimeter- (1- by 1- by 3-in.-) samples for orientations perpendicular to the direction of foam rise

Apparatus

Tensile and compression tests. - Standard laboratory precision hydraulic testing machines were utilized for all tensile and compressive tests of foam samples. For all tests except those conducted at liquid hydrogen temperatures, a testing machine having a 0- to 2220-newton (0- to 500-lb) range (overall accuracy, ±0.5 percent of full scale) was used. A specially modified testing machine having a 0- to 222-newton (0- to 50-lb) range (overall accuracy ±0.5 percent of full scale) was utilized for all tests conducted at liquid hydrogen temperature.

Shear modulus tests. - The foam samples were mounted on a fixed base and subjected to a torque by means of a precalibrated wire shaft which was carefully alined with the centerline of the sample. Since the shear modulus of the wire shaft was known, the shear modulus of the foam could then be determined by noting the relative angular rotation between the foam sample and the wire shaft when subjected to a torque.

Thermal contraction tests. - The base of the foam sample was held fixed while the movement (thermal contraction) of the top of the sample was determined by means of a dial indicator.

The foam sample for each of the tests noted previously was bonded between mounting blocks (either aluminum or plastic) with an adhesive suitable for the temperatures at which each specific test was conducted. To obtain temperatures below ambient room

temperature, the sample was mounted in the test fixture and enclosed by a small cylindrical tank. The sample was then immersed in a fluid, and the temperature of the sample was determined from the following:

(1) Temperatures of liquid hydrogen and liquid nitrogen for saturated conditions at atmospheric pressure

(2) Temperature of alcohol with and without dry ice as measured by a mercury thermometer

Test Results

Compression tests. - The results indicated that the yield strength (fig. 18) and modulus of elasticity (fig. 19) were greater in the direction parallel to the foam rise and that the strength and modulus generally increased with decreasing temperature. The results generally agree with the data presented in reference 10. The faired curves indicate the trends which were utilized in the computer program to predict the thermal stresses in the foam insulation on tank 3.

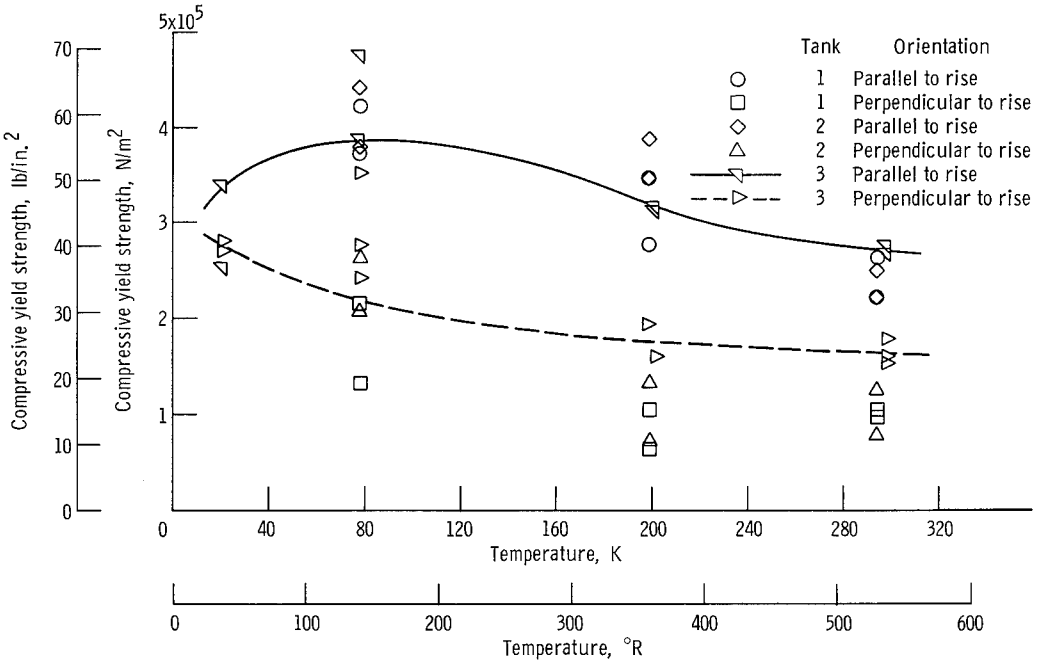

Figure 18. - Compressive yield strength.

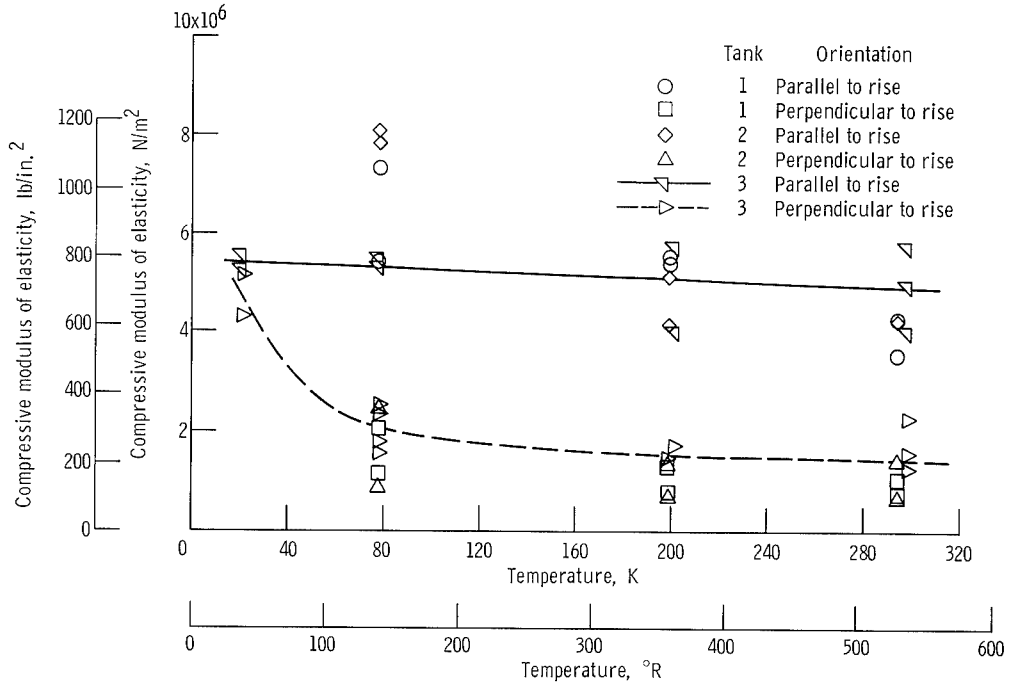

Figure 19. - Compressive modulus of elasticity.

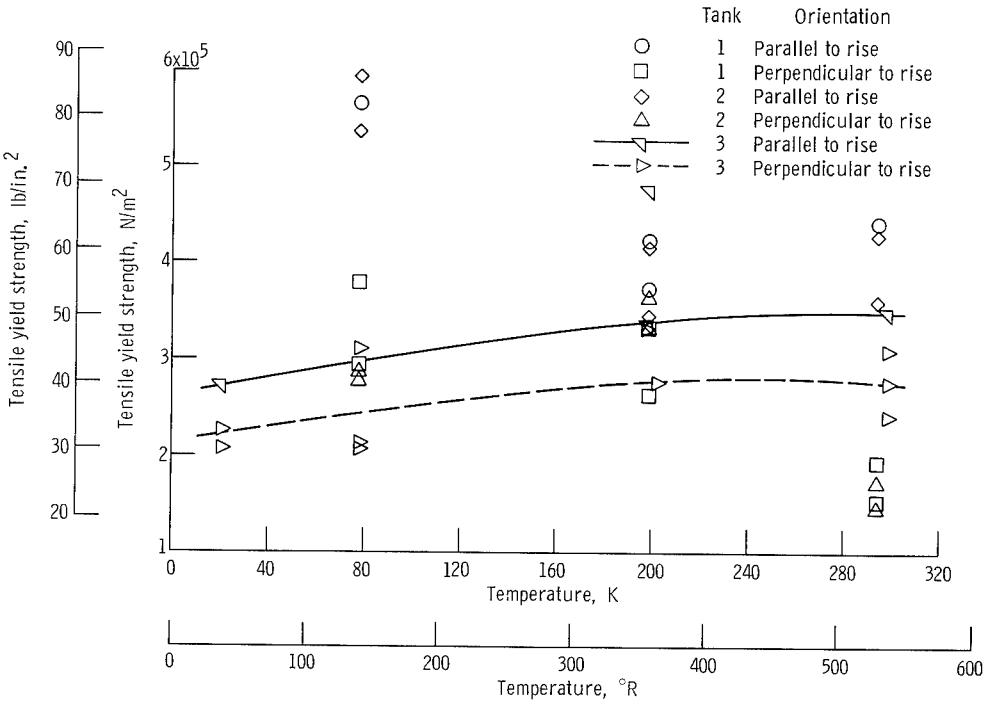

Figure 20. - Tensile yield strength.

Tension tests. - The results indicated that the yield strength (fig. 20) and modulus of elasticity (fig. 21) were again greater in the direction parallel to the foam rise. The yield strength decreased, while the modulus of elasticity increased slightly with decreasing temperature for the foam on tank 3. A large degree of data scatter can be noted between the results from foam samples for tanks 1 and 2 and the results for tank 3 in the direction parallel to the foam rise, particularly at liquid nitrogen temperatures. The reason for this is not specifically known since (1) the results for all tanks generally showed good agreement for the compression testing and (2) even though the foam sample

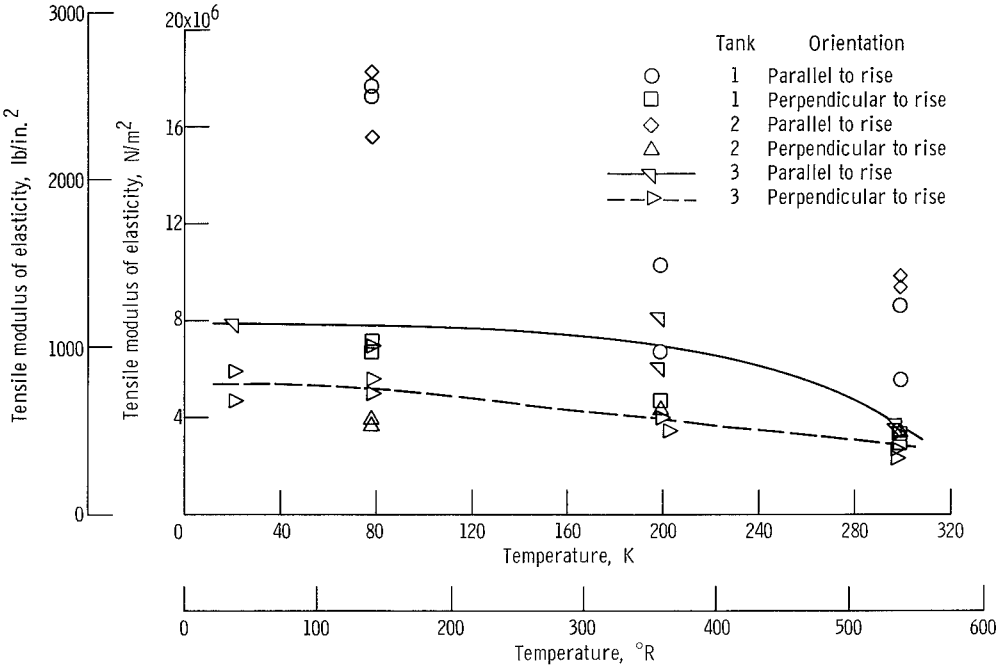

Figure 21. - Tensile modulus of elasticity.

lengths were different (2.5 cm or 1.0 in. for tank 3 as compared with 7.6 cm or 3.0 in. for tanks 1 and 2), the foam fractured near the center of each sample. The faired curves again indicate the trends utilized in the computer program to predict thermal stresses.

Shear tests. - The results of the tests to determine the shear modulus of the foam insulation are shown in figure 22. The shear modulus (1) increased with decreasing temperature and (2) showed no distinct or consistent differences between parallel and perpendicular orientation to the foam rise. The results shown were similar to that

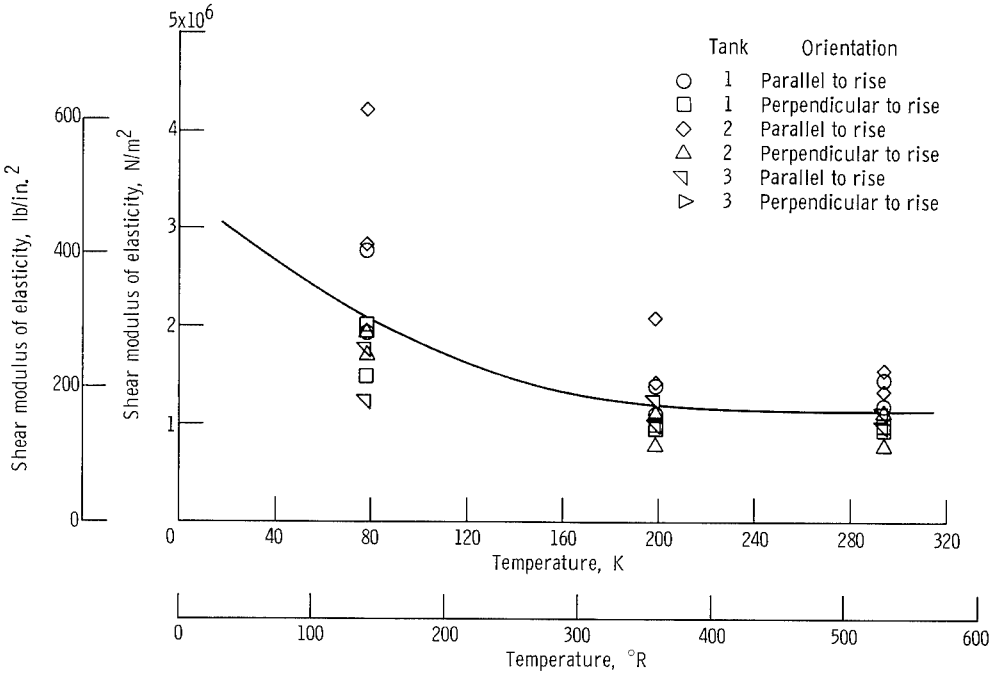

Figure 22. - Shear modulus of elasticity.

noted in reference 10 except that the values shown in figure 22 are somewhat lower.

Thermal contraction tests. - The results, shown in figure 23, indicated that the thermal contraction was greater in the orientation perpendicular to the foam rise than parallel to the foam rise. These results are consistent with those noted in reference 10. The data generally did not show too much scatter although, in two instances, there were considerable differences noted between the foam on the top and bottom halves of the tank. The faired curves indicate the values of thermal contraction utilized in obtaining the coefficient of thermal contraction for the computer program to predict thermal stresses.

Discussion

The thermophysical properties of the foam samples obtained for tank 3 tended to show closer agreement between orientation parallel and perpendicular to the direction of foam rise when compared to the first two tanks. This trend, coupled with the foaming-in-place technique is believed responsible for the structural integrity of the foam insulation on tank 3 throughout all of the experimental testing.

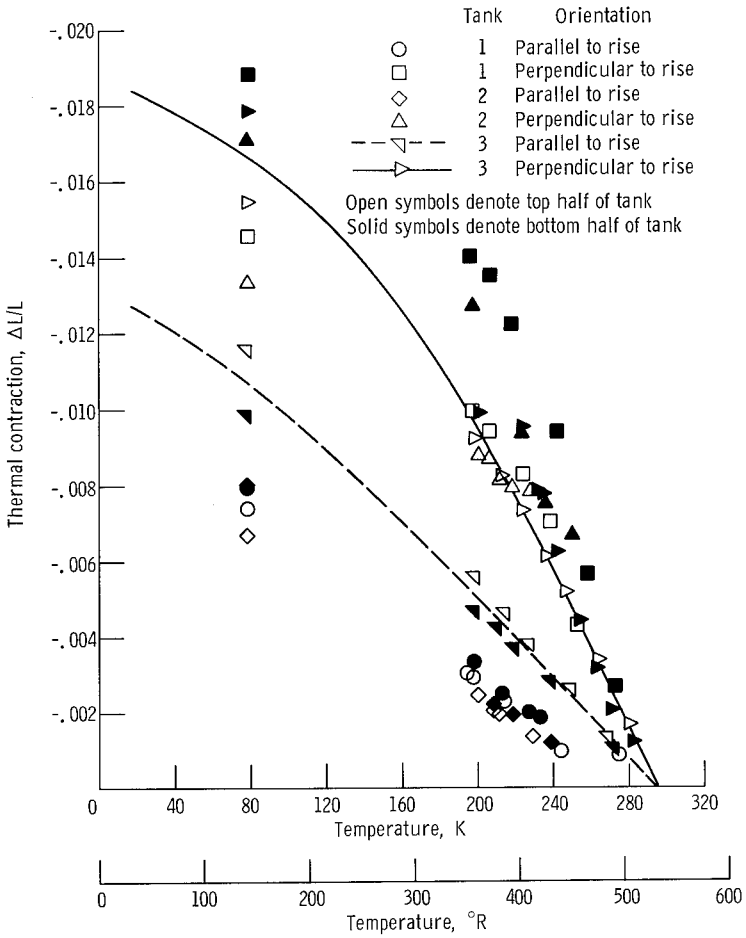

Figure 23. - Thermal contraction.

APPENDIX C

ANALYTICAL THERMAL STRESS CALCULATIONS

To complete the investigation reported herein, it was desirable to analytically predict the stress profiles occurring within the layer of foam insulation for several of the temperature profiles obtained during the experimental phase of the testing. The stresses occurring within the insulation are thermal stresses resulting from the higher rate of thermal contraction of the foam when compared to that of the tank wall. It would be expected, then, that compressive stresses would occur in the radial direction and tensile stresses would occur in the tangential direction to the tank wall. Also, it was desirable to analytically determine the effect of tank size and foam insulation thickness on the predicted stress levels.

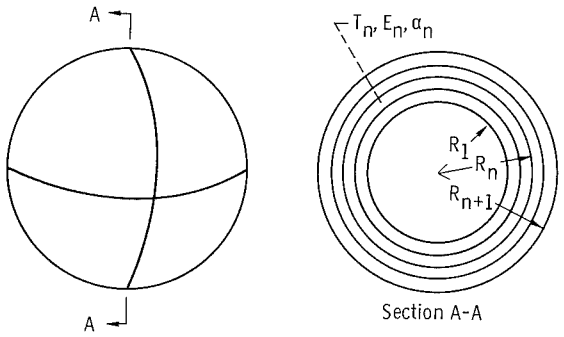

(a) Concentric n-layer spherical shell.

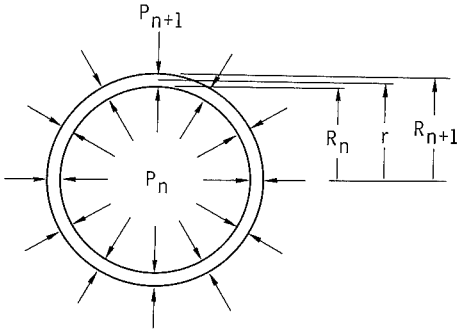

(b) Free body diagram of n^{th} concentric layer.

Figure 24. - Analytical model for stress analysis.

Mathematical Model

The layer of foam insulation, together with the tank wall, was assumed to be composed of n concentric, spherical shells (fig. 24) as described in reference 8. Each shell was considered to be elastic, homogeneous, and isotropic. Temperature profiles obtained experimentally from the chilldown tests for both ground-hold and space-hold conditions were used in the mathematical model. The temperature of each shell was assumed to be uniform across the shell and equal to the mean temperature as determined from the experimentally measured temperature profile. A total of 51 concentric shells were utilized in the computer program, with the tank wall being the inner shell and the foam layer being composed of 50 shells.

The radial stress for the n^{th} shell was determined from the following equation (ref. 8):

$$\sigma_{r_n} = \frac{R_n^3 R_{n+1}^3 \left(P_{n+1} - P_n\right)}{\left(R_{n+1}^3 - R_n^3\right) r^3} + \frac{P_n R_n^3 - P_{n+1} R_{n+1}^3}{R_{n+1}^3 - R_n^3}$$

$$+ \frac{2\alpha_n E_n}{1 - \nu_n} \left[\frac{r^3 - R_n^3}{\left(R_{n+1}^3 - R_n^3\right) r^3} \int_{R_n}^{R_{n+1}} Tr^2 dr - \frac{1}{r^3} \int_{R_n}^{r} Tr^2 dr \right]$$

The tangential stress for the n^{th} shell was determined from the following equation (ref. 8):

$$\sigma_{\theta_n} = - \frac{R_n^3 R_{n+1}^3 \left(P_{n+1} - P_n\right)}{\left(R_{n+1}^3 - R_n^3\right) 2r^3} + \frac{P_n R_n^3 - P_{n+1} R_{n+1}^3}{R_{n+1}^3 - R_n^3}$$

$$+ \frac{2\alpha_n E_n}{1 - \nu_n} \left[\frac{2r^3 + R_n^3}{2\left(R_{n+1}^3 - R_n^3\right) r^3} \int_{R_n}^{R_{n+1}} Tr^2 dr + \frac{1}{2r^3} \int_{R_n}^{r} Tr^2 dr - \frac{T_r}{2} \right]$$

T

The interface pressures are determined from the boundary condition and the following equation:

$$W_n P_n + X_n P_{n+1} + Y_n P_{n+2} = Z_n \qquad (n = 1, 2, 3, \ldots, N - 1)$$

where

$$W_n = \frac{3(1 - \nu_n)\left(R_{n+2}^3 - R_{n+1}^3\right)R_n^3}{E_n}$$

$$X_n = -\left\{\frac{1}{E_n}\left(R_{n+2}^3 - R_{n+1}^3\right)\left[(1 + \nu_n)\, R_n^3 + 2(1 - 2\nu_n)R_{n+1}^3\right]\right.$$

$$\left. + \frac{1}{E_{n+1}}\left(R_{n+1}^3 - R_n^3\right)\left[(1 + \nu_{n+1})R_{n+2}^3 + 2(1 - 2\nu_{n+1})\, R_{n+1}^3\right]\right\}$$

$$Y_n = \frac{3(1 - \nu_{n+1})\left(R_{n+1}^3 - R_n^3\right)R_{n+2}^3}{E_{n+1}}$$

and

$$Z_n = 6\alpha_{n+1}\left(R_{n+1}^3 - R_n^3\right)\int_{R_{n+1}}^{R_{n+2}} Tr^2 dr - 6\alpha_n\left(R_{n+2}^3 - R_{n+1}^3\right)\int_{R_n}^{R_{n+1}} Tr^2 dr$$

The assumptions for the analysis included the following:

(1) T_r = temperature at which foam insulation was allowed to set and cure on the tank (approx 322 K or 580° R).

(2) P_1 = tank pressure.

(3) P_N = environmental pressure.

The analysis accounts for both temperature and material dependent properties from shell to shell but does not account for variations of properties in the tangential and radial directions (perpendicular and parallel to the direction of foam rise, respectively). In the program, the interface pressures P_n were calculated using the radial (parallel to rise) foam properties; then the tangential and radial stresses were calculated using the tangential and radial foam properties, respectively. Generally, the use of the computer program in this manner should provide results of sufficient accuracy for engineering purposes. Also, since the foam is not really isotropic, the use of Poisson's ratio is not exactly correct either. For the purpose of this investigation, however, a value of Poisson's ratio of 0.41 was assumed (ref. 11).

The temperature profiles imposed on the foam insulation were averages of the experimentally measured temperatures obtained at various times during the chilldown tests on the top and bottom halves of tank 3 for both ground-hold and space-hold conditions, test 1 (fig. 13) and test 7 (fig. 17), respectively. The test times of the temperature profiles as well as the foam properties utilized in the computer program are shown in table V.

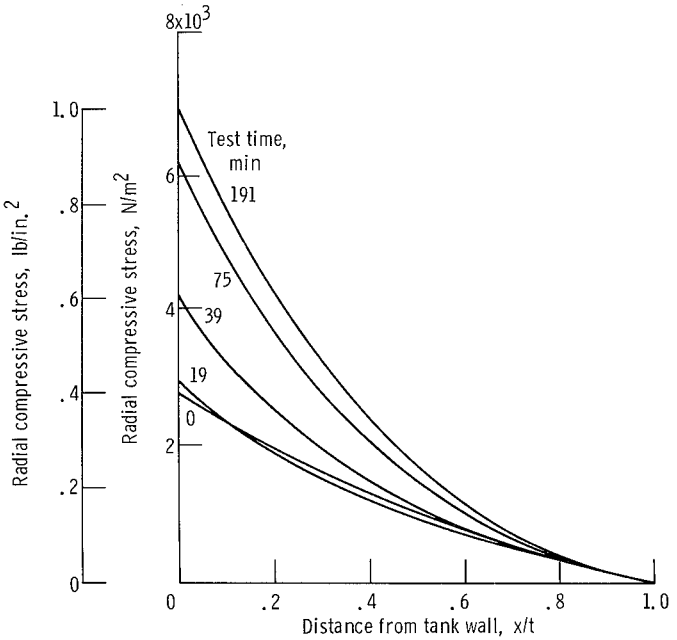

Figure 25. - Predicted foam radial stress profiles for tank 3, test 1 (ground-hold conditions).

Results

The analytically predicted radial and tangential stresses within the layer of foam insulation for the ground-hold test (test 1) of tank 3 are shown in figures 25 and 26, respectively. The radial stresses indicated compressive loadings and the tangential stresses indicated tensile loadings as would be expected since the foam insulation has a higher rate of contraction than the aluminum tank wall. The highest stresses are found adjacent to or near the tank wall-foam interface. The stresses generally tend to increase as the temperature gradient across the foam insulation increased. In all cases, however,

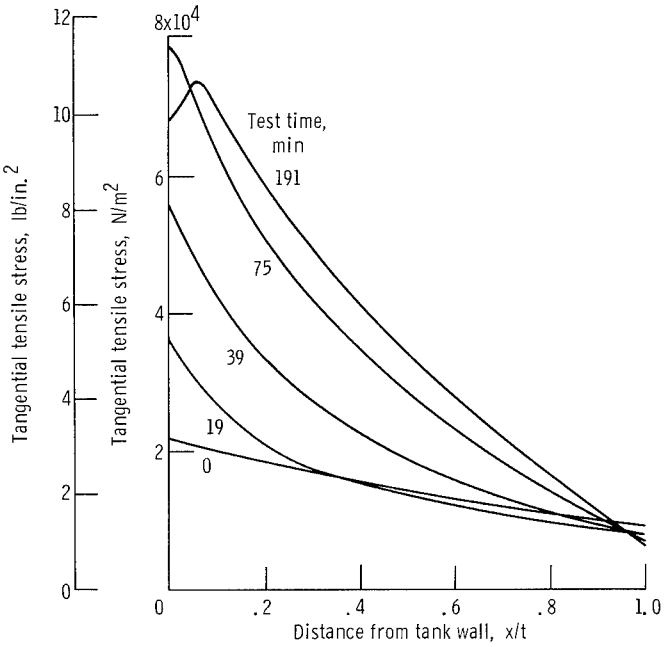

Figure 26. - Predicted foam tangential stress profiles for tank 3, test 1 (ground-hold conditions).

the predicted foam stresses were well below the yield strengths noted in the foam sample tests.

The analytically predicted radial and tangential stresses for the space-hold test (test 7) of tank 3 are shown in figures 27 and 28, respectively. The somewhat strange behavior of the stresses occurring during the transition from ambient temperature to liquid hydrogen temperature is caused by the liquid hydrogen cooled shroud which cooled down the outside of the foam insulation layer more rapidly than the interior of the layer. The predicted stresses at the end of the space-hold test were generally more severe than for the ground-hold test but still well below the yield strengths noted in the foam sample testing.

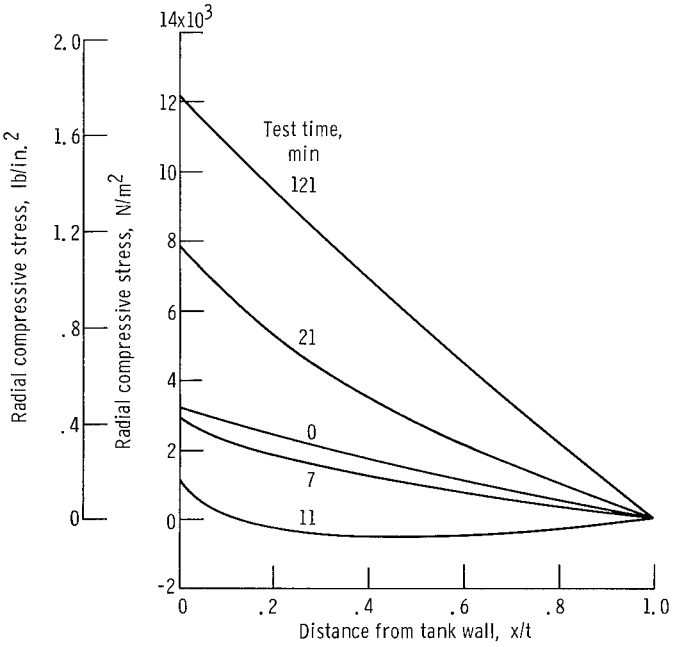

Figure 27. - Predicted foam radial stress profiles for tank 3, test 7 (space-hold conditions).

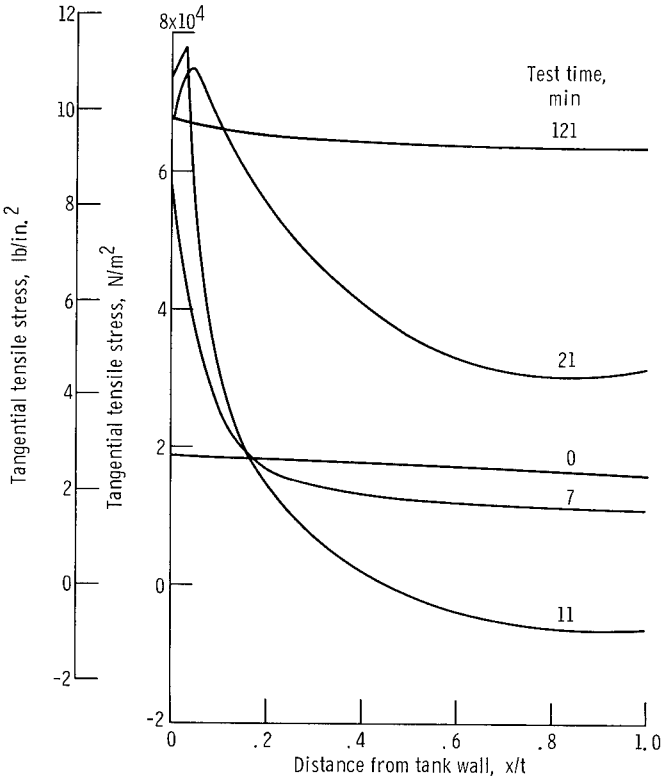

Figure 28. - Predicted foam tangential stress profiles for tank 3, test 7 (space-hold conditions).

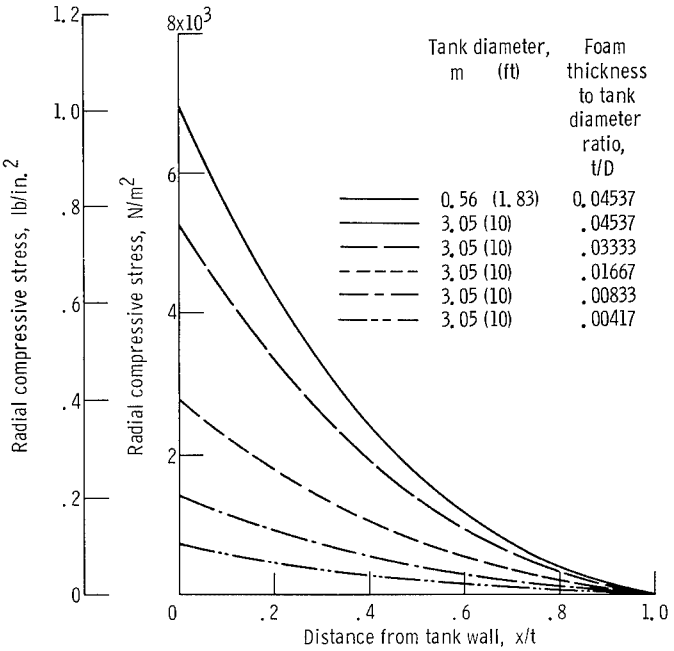

Figure 29. - Predicted foam radial stress profiles for varying foam thickness.

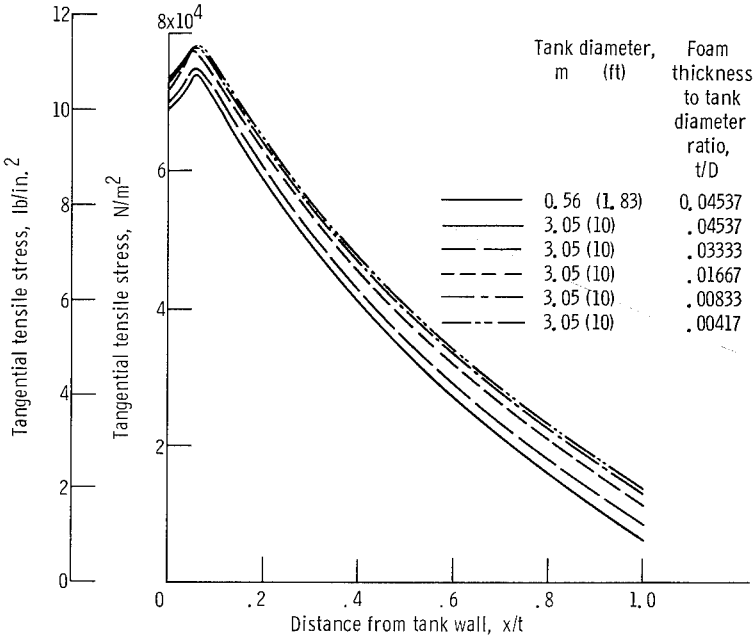

Figure 30. - Predicted foam tangential stress profiles for varying foam thickness.

The analytically predicted stresses within the foam insulation for tanks of varying size are shown in figures 29 and 30 for the radial and tangential stresses, respectively. To illustrate the effect of tank size, a spherical tank having a diameter of 3.05 meters (10 ft) was arbitrarily chosen. The average temperature profile obtained at a test time of 191 minutes for ground-hold test 1 of tank 3 (fig. 13) was generalized with respect to the distance from the tank wall x/t to account for varying foam insulation thickness and then applied to several insulation thicknesses. This simplifying assumption used together with the analytical results indicated that the generalized stress profiles were identical for tanks of varying size if the values of the foam thickness to tank diameter ratio t/D were equal. In addition, the analytical results indicated that the radial compressive stresses decreased, and the tangential tensile stresses increased only slightly, as the foam thickness to tank diameter ratio decreased.

REFERENCES

1. Dearing, D. L.: Development of the Saturn S-IV and S-IVB Liquid Hydrogen Tank Internal Insulation. Advances in Cryogenic Engineering. Vol. 11. K. D. Timmerhaus, ed., Plenum Press, 1966, pp. 89-97.

2. Hammond, M. B., Jr.: Liquid Hydrogen Tank Insulation for the S-11 Booster. Chem. Eng. Progr. Symp. Ser., vol. 62, no. 61, 1966. pp. 213-218.

3. Lewis Research Center Staff: Sealed-Foam, Constrictive-Wrapped, External Insulation System for Liquid-Hydrogen Tanks of Boost Vehicles. NASA TN D-2685, 1965.

4. Sterbentz, W. H.; and Baxter, J. W.: Thermal Protection System for a Cryogenic Spacecraft Propulsion Module, Vol. II. Rep. LMSC-A794993, vol. 2, Lockheed Missiles and Space Co. (NASA CR-54879, vol. 2), Nov. 15, 1966.

5. Black, Igor A., et al.: Basic Investigation of Multi-layer Insulation Systems. Rep. ADL-65958-00-04, Arthur D. Little, Inc. (NASA CR-54191), Oct. 30, 1964.

6. Haskins, J. F.; and Hertz, J.: Thermal Conductivity of Plastic Foams from -423° to 75° F. Advances in Cryogenic Engineering. Vol. 7. K. D. Timmerhaus, ed., Plenum Press, 1962, pp. 353-359.

7. Saunders, J. H.; and Frisch, K. C.: Polyurethanes: Chemistry and Technology. Part II. John Wiley & Sons, Inc., 1964, p. 253.

8. Au, Norman N.: Stresses and Strains in Multi-layer Disks, Cylinders, and Spheres Under Pressure Loading and an Arbitrary Radial Temperature Gradient. Rep. TDR-269(4304)-2, Aerospace Corp. (AFSSD-TDR-63-227), Oct. 31, 1963.

9. Kaufman, Albert: Investigation of Strain Gages for Use at Cryogenic Temperatures. Experimental Mech., vol. 3, no. 8, Aug. 1963, pp. 177-183.

10. Sweet, H. S.; and Steele, A. J.: Insulation Materials Handbook. Rep. LMSC/A709158, Lockheed Missiles and Space Co. (NASA CR-59622), 1964.

11. McClintock, R. M.: Mechanical Properties of Insulating Plastic Foams at Low Temperatures. Advances in Cryogenic Engineering. Vol. 4. K. D. Timmerhaus, ed., Plenum Press, 1960, pp. 132-140.

TABLE I. - CONSTITUENTS OF FOAM FORMULATIONS

Constituent	Parts by weight	
	Tanks 1 and 2	Tank 3
Plaskon PFR 6 foam resin	100.0	100.0
Dabco LV-33 catalyst	.6	.6
Union Carbide 5310 silicone surfactant	1.5	1.5
Glidden RCR 5043 isocyanate prepolymer	111.0	---
Nadconate 1080 HM prepolymer	----	110.0
Freon R-11 fluorocarbon blowing agent	30.0	26.5

TABLE II. - EXPERIMENTAL TEST PROGRAM FOR FOAM INSULATED TANKS

Tank	Test	Type of test	Chilldown rate		Foam insulation surface temperature with liquid hydrogen filled tank		Thermal conductivity		Remarks
			K/min	^{o}R/min	K	^{o}R	W/(m)(K)	Btu/(hr)(ft)(^{o}R)	
1	1	Chilldown and boiloff	1.1	1.98	265	477	0.0150	0.0087	Noted severe wrinkling of vapor barrier and deep indentations in foam around equator of tank during chilldown
2	1	Chilldown and boiloff	0.53 to 1.18	0.96 to 2.12	270	486	.0165	.0095	
	2	↓	2.09	3.76	274	493	.0126	.0072	
	3		8.76	15.96	270	486	.0144	.0083	
	4		26.7	48.1	274	493	.0148	.0085	
	5	Chilldown	4.93	8.87	275	495	------	------	Facility checkout prior to testing tank 3; mylar/aluminum/aluminum/mylar vapor barrier removed and foam coated with G-207 adhsesive for tests 5 to 7
	6	Space hold	20.5	36.9	234	421	------	------	
	7	Space hold	68	122	---	---	------	------	Tank insulated with six layers single-aluminized mylar; cracks noted in foam near equator of tank after test; thermocouple leads severed or strained
3	1	Chilldown and boiloff	2.23	4.01	268	482	.0138	.0080	Only slight amount of wrinkling of vapor barrier and one slight indentation encircling tank at equator
	2	↓	10.2	18.4	272	490	.0137	.0079	
	3		21.0	37.8	276	497	.0135	.0078	
	4	Vibration	----	----	292	526	------	------	
	5	Space hold	40.6	73.1	140	252	------	------	Tank insulated with six layers single-aluminized mylar
	6	↓	47.0	84.6	95.4	172	------	------	
	7		31.6	56.9	41.9	75	------	------	Tank insulated with six layers single-aluminized mylar; tank also enclosed within liquid hydrogen cooled shroud

TABLE III. - RESISTANCE RATIOS FOR

FOAM THERMOCOUPLE PROBES

Probe length		Resistance ratio, g/g_T	Remarks
cm	in.		
2.54	1.00	0.0585	Initial calibration
2.22	.88	.0668	Foam insulated tank 3
1.90	.75	.0780	↓
1.27	.50	.1170	
.63	.25	.2339	

TABLE IV. - FOAM INSULATED TANK 3 VIBRATION TEST CONDITIONS

Time interval, sec	Static load		Overall tank and insulation static deflection		Vibratory load[a]		Vibratory frequency, Hz	Overall tank and insulation vibratory deflection[a]		Temperature conditions
	N/m^2	psi	cm	in.	N/m^2	psi		cm	in.	
200	10.65×10^4	15.4	0.251	0.099	0	0	0	0	0	Ambient temperature (298 K or 536° R)
127	11.10	16.1	.248	.098	$.17\times10^4$	.2	5.00	.004	.0016	
42.6	10.36	15.0	.243	.096	2.95	4.3	9.85	.020	.0080	
35.0	10.65	15.4	.221	.087	1.57	2.3	14.70	.029	.0116	
36.7	10.50	15.2	.217	.086	1.04	1.5	19.50	.015	.0060	
39.3	10.36	15.0	.220	.087	.71	1.0	29.50	.014	.0056	
64.0	10.43	15.1	.225	.089	3.43	5.0	4.97	.015	.0058	
31.9	10.39	15.1	.237	.093	3.23	4.7	9.80	.029	.0116	
34.1	10.50	15.2	.243	.096	2.35	3.4	14.75	.033	.0130	
34.9	10.21	14.8	.239	.094	1.83	2.7	19.50	.029	.0116	
35.8	10.43	15.1	.257	.101	4.36	6.3	29.45	.039	.0154	
34.5	10.54	15.3	.239	.094	4.99	7.2	5.00	.047	.0186	
52.5	10.80	15.7	.246	.097	6.79	9.8	9.82	.040	.0158	
35.2	10.43	15.1	.244	.096	4.77	6.9	14.70	.030	.0120	
42.1	10.36	15.0	.239	.094	7.71	11.2	19.60	.045	.0176	
34.9	10.32	15.0	.234	.092	4.14	6.0	29.50	.024	.0094	
67.0	10.36	15.0	.254	.100	7.78	11.3	5.00	.050	.0195	
34.5	10.65	15.4	.264	.104	7.33	10.6	9.84	.048	.0188	
32.9	10.47	15.2	.264	.104	7.10	10.3	14.68	.039	.0152	
34.1	10.54	15.3	.267	.105	7.63	11.1	19.58	.052	.0204	
36.3	10.50	15.2	.267	.105	6.74	9.8	29.42	.042	.0166	
34.5	10.88	15.8	.262	.103	10.85	15.7	5.00	.075	.0296	
34.1	10.61	15.4	.257	.101	11.94	17.3	9.81	.082	.0324	
35.2	10.58	15.3	.262	.103	11.16	16.2	14.68	.068	.0268	
38.2	10.81	15.7	.269	.106	11.70	17.0	19.59	.081	.0320	
37.2	10.28	14.9	.262	.103	10.92	15.8	29.44	.069	.0271	
-----	0	0	.196	.077	0	0	0	0	0	

-----	0	0	0.130	0.051	0	0	0	0	0	Tank filled with liquid hydrogen
33.5	10.17×10^4	14.7	.241	.095	$.45\times10^4$	.7	5.00	.006	.0024	
33.6	10.43	15.1	.241	.095	.28	.4	9.80	.005	.0018	
34.4	10.43	15.1	.244	.096	.37	.5	14.67	.005	.0020	
33.7	10.59	15.4	.236	.093	1.94	2.8	19.62	.009	.0036	
36.7	10.43	15.1	.213	.084	.93	1.3	29.42	.014	.0055	
-----	0	0	.152	.060	0	0	0	0	0	
39.0	10.36	15.0	.178	.070	2.41	3.5	5.00	.022	.0088	
37.6	10.74	15.6	.185	.073	2.71	3.9	9.81	.025	.0078	
33.9	10.77	15.6	.188	.074	2.89	4.2	14.70	.041	.0162	
35.8	10.43	15.1	.173	.068	2.78	4.0	19.58	.065	.0256	
11.2	9.84	14.3	.168	.066	3.96	5.7	30.56	.077	.0303	
15.4	9.84	14.3	.345	.136	18.93	27.4	29.50	.242	.0954	
15.0	3.79	5.5	.323	.127	2.82	4.1	4.97	.014	.0056	
32.5	10.47	15.2	.368	.145	4.46	6.5	4.97	.021	.0083	
33.6	10.28	14.9	.368	.145	4.68	6.8	9.82	.025	.0098	
36.2	10.39	15.1	.366	.144	4.53	6.6	14.70	.023	.0092	
1.8	10.39	15.1	.384	.151	21.57	31.3	19.58	.191	.0750	
34.2	10.43	15.1	.371	.146	4.79	6.9	19.58	.026	.0104	
35.0	10.36	15.0	.368	.145	6.09	8.8	29.55	.035	.0138	
39.3	10.43	15.1	.368	.145	8.17	11.8	4.99	.046	.0180	
4.1	7.21	10.5	.356	.140	15.07	21.9	9.81	.161	.0634	
32.7	10.50	15.2	.427	.168	7.66	11.1	9.81	.046	.0180	
35.2	10.32	15.0	.424	.167	7.94	11.5	14.70	.045	.0176	
37.5	10.50	15.2	.422	.166	8.28	12.0	19.59	.050	.0196	
36.5	10.92	15.8	.427	.168	8.54	12.4	28.00	.051	.0200	
-----	11.32	16.4	.437	.172	0	0	0	0	0	
-----	0	0	.348	.137	0	0	0	0	0	
-----	0	0	.279	.110	0	0	0	0	0	
-----	10.17	14.7	.424	.167	0	0	0	0	0	
30.5	10.43	15.1	.422	.166	10.92	15.8	5.00	.078	.0308	
33.7	10.06	14.6	.417	.164	9.51	13.8	9.82	.056	.0219	
34.2	10.28	14.7	.422	.166	9.88	14.3	14.67	.064	.0252	
36.3	10.39	15.1	.427	.168	11.21	16.3	19.55	.071	.0278	
35.8	10.17	14.7	.424	.167	9.88	14.3	29.50	.053	.0208	
-----	10.63	15.4	.437	.172	0	0	0	0	0	
-----	1.45	2.1	.368	.145	0	0	0	0	0	
-----	0	0	.312	.123	0	0	0	0	0	

[a]Peak to peak.

TABLE V. - INPUTS TO COMPUTER PROGRAM TO PREDICT STRESS PROFILES WITHIN LAYER OF FOAM INSULATION FOR TANK 3

Temperature profile		Modulus of elasticity		Thermal contraction		Tank pressure		Tank radius		Insulation thickness	
Test	Time, min	Radial	Tangential	Radial	Tangential	N/m^2	psi	cm	in.	cm	in.
1	0	Compression[a]	Tension[b]	(a)	(b)	3220	0.54	27.99	11.01	2.54	1.00
	19	↓	↓	↓	↓	↓	↓	↓	↓	↓	↓
	39										
	79										
	191										
7	0					10^5	14.54				
	7					↓	↓				
	11										
	21										
	121										
1	191					3220	.54	152.4	60	13.83	5.45
	↓					↓	↓	↓	↓	10.16	4.0
										5.08	2.0
										2.54	1.0
										1.27	.5

[a] Parallel to foam rise.

[b] Perpendicular to foam rise.